HERON contains contributions based mainly on research work performed in I.B.B.C. and STEVIN and related to strength of materials and structures and materials science.

Jointly edited by:

STEVIN-LABORATORY
of the Department of
Civil Engineering of the
Technological University, Delft,
The Netherlands
and
I.B.B.C. INSTITUTE TNO
for Building Materials
and Building Structures,
Rijswijk (ZH), The Netherlands.

EDITORIAL STAFF:

F. K. Ligtenberg, *editor in chief*
M. Dragosavić
H. W. Loof
J. Strating
J. Witteveen

Secretariat:

L. van Zetten
P.O. Box 49
Delft, The Netherlands

HERON

vol. 20
1974
no. 1

Contents

A DESIGN METHOD FOR THE TENSION SIDE OF STATICALLY LOADED, BOLTED BEAM-TO-COLUMN CONNECTIONS

P. Zoetemeijer
(STEVIN LABORATORY)

Summary 3
Samenvatting 3
Acknowledgment 4
0 **Introduction** 5
1 **A design method for T-stub connections** . 8
1.1 Introduction 8
1.2 Collapse mechanism A 10
1.3 Collapse mechanism B 11
1.4 Adaptation to limit state design . . 13
2 **A design method for T-stub flange to column connections** 14
3 **The effective length of the column flange** . 17
3.1 Method of calculation 17
3.2 Limit analysis of collapse mechanisms I and II 18
3.2.1 Collapse mechanism I 18
3.2.2 Collapse mechanism II . . . 25
3.2.3 The effective length 32
3.3 The influence of stiffening plates . . 34
4 **Test results** 38
4.1 Tests to check *T*-stub design 38
4.2 Tests to check the effective length . 39
4.3 Tests to check *T*-stub flange to column connection design 43
5 **Deformations** 46
6 **Tests to check the deformation limitations** 47
6.1 Introduction 47
6.2 Explanation to the results mentioned in table IV and V 48
6.4 Additional tests 53
7 **Concluding remarks** 59

Notations

A_s	stress area
B	bolt force
$\Sigma \hat{B}_t$	total limit load of the bolts fitted at one side of a T-stub to column connection
ΣB_u	total ultimate tensile load of the bolts fitted at one side of a T-stub to column connection
ΔE	internal dissipation of energy during an assumed plastic deflection
F_t	limit load of a construction in tension
M_p	plastic moment that causes a plastic hinge to form immediately adjacent to the tensile strip of a T-stub and at a distance of $0.8 \times$ the fillet radius from the column web
M'_p	plastic moment that causes a plastic hinge to form at the bolt line
M_{vt}	theoretical yield moment of a beam to column connection obtained by using design formulas
Q	prying action between the flange plates of column and/or T-stubs
$Q_{\max}$	maximum value of the prying action
T	half of the design load of a T-stub to column connection
T_u	half of the ultimate tensile load applied to a T-stub to column connection
ΔT	work done by the external loads during an assumed plastic deformation
a	distance between the center lines of adjacent bolt holes measured parallel to the plane of the web of a column or T-stub
b	width of the flange plate which contributes to load transmission
d	bolt diameter
m	distance from the location of M_p to the bolt line
m_k	same as m but only for column flange design
m_f	same as m but only for T-stub flange design
m_p, m_{p1}	yield moment per unit length of the flange
m_{p2}	yield moment per unit length of the stiffening plate bolted parallel to the flange
n	distance from the bolt line to the location of the prying action assumed at the outer edge of the flange plate or at a distance equal to $1{,}25 \times m$, if it is smaller
n'	distance from the bolt line to the outer edge of the flange plate in the same direction as n
n_f, n_k	same as n but for T-stub or column flange design, respectively
r	radius
t, t_f	thickness of the flange plate
σ_e	yield stress of the material
σ_t	tensile stress of the material
α, β	angle

A DESIGN METHOD FOR THE TENSION SIDE OF STATICALLY LOADED, BOLTED BEAM-TO-COLUMN CONNECTIONS

Summary

In this paper a design method for the tension side of statically loaded, bolted beam-to-column connections is developed based on the plastic behaviour of the flanges and the bolts under the assumption that the plastification is large enough to allow the adoption of the most favourable static equilibrium.

Until now bolted beam-to-column connections without stiffening plates welded between the column flanges have been generally avoided.

The reason for this is that the deformations of the connection are considerable and, until now, a formula which allows the determination of the stiffness and strength of a column flange has been lacking.

This paper presents the derivation of an "effective" length formula for a column flange in tension without stiffening plates between the flanges. The derivation is based on the analysis of two different collapse mechanisms.

One mechanism occurs if bolt failure governs collapse. The other mechanism corresponds to collapse resulting from the full plastification of the column flanges.

Tests are discussed that were performed to insure that the developed design rules would lead to connections that would satisfy the limit state of deformations as given in the Dutch regulations for constructional steel work (for both) serviceability and ultimate limit states.

Samenvatting

In dit artikel wordt een ontwerpmethode ontwikkeld voor de trekzijde van niet dynamisch belaste geboute balk-kolomverbindingen. De methode is gebaseerd op het plastisch gedrag van de flenzen en de bouten, er van uitgaande dat een bezwijkmechanisme kan ontstaan en de laagste belasting uit een evenwichts- of arbeidsbeschouwing volgt.

Tot op dit moment wordt het toepassen van balk-kolomverbindingen zonder gelaste schotten tussen de kolomflenzen vermeden. De reden hiervoor is, dat de vervormingen van de verbinding aanzienlijk zijn en verder dat een formule waarmee de sterkte en stijfheid van een kolomflens kan worden berekend ontbreekt.

Dit artikel geeft de afleiding van een formule voor de medewerkende lengte van een kolomflens aan de getrokken zijde van een geboute balk-kolomverbinding zonder gelaste schotten tussen de flenzen.

De afleiding is gebaseerd op de bezwijkanalyse van twee verschillende bezwijkmechanismen.

Een mechanisme ontstaat als boutbreuk tot bezwijken leidt, het andere als de bout zo sterk is dat de flenzen volledig vloeien. Proeven worden besproken die zijn uit-

gevoerd om na te gaan of de ontwikkelde ontwerpregels verbindingen geven die aan de sterkte- en stijfheidseisen volgens de T.G.B. 1972-Staal voldoen, zowel in het gebruik als in het bezwijkstadium.

Acknowledgment

The method of design developed in this paper was initiated by ir. J. de Back who also guided the research project. His many suggestions during the writing of this paper has been of great value.

The analysis of the proposed collapse mechanisms has been done by ir. W. A. J. Tromp.

Discussions in the Committee "Hoekverbindingen" of the "Staalbouwkundig Genootschap" (Committee on beam to column connections of the Netherlands Society of Steel Construction) have been of great help in the derivation of the design rules. The suggestion to check the proposed rules with respect to the limit states of deformations as given in the Dutch regulations has also been made by this Committee.

All tests were executed at the Stevin Laboratory of the Delft University of Technology. The majority of the tests were performed by students as a part of their education as a civil engineer.

A design method for the tension side of statically loaded, bolted beam-to-column connections

0 Introduction

Steel framework often contains connections with bolts loaded by tensile forces due to external loads.

In the following figures some of these connections are shown.

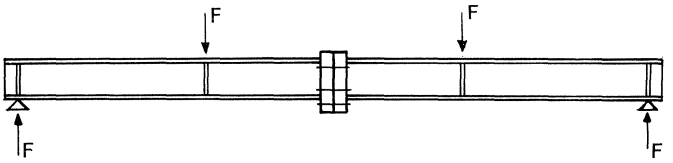

Fig. 0.1. End plate connection in a beam.

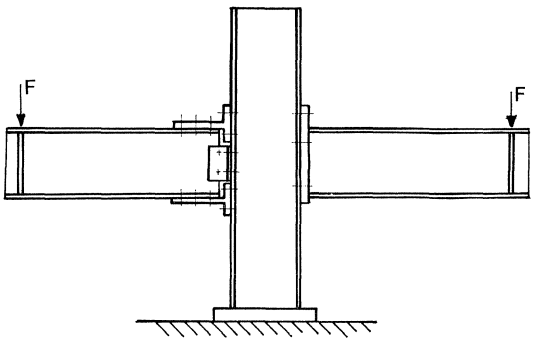

Fig. 0.2. T-stub and end plate beam-to-column connection.

In the end plate connection of figure 0.1 the bolts near the lower flange are subjected to tensile forces, while in figure 0.2 the upper flange is the tension side of the beam.

A less complicated and simplified connection, which shows the same behaviour as the connection given in figure 0.2 is drawn in figure 0.3 (T-stub connection). An applied load of $2T$ is to be transmitted. At first glance it might seen that each bolt in this connection will transmit a load $2T/2 = T$.

In practice, the external load of this connection will bend the T-stub flange (see figure 0.4). This deflection will cause the flanges to exert pressure on each other. The result is that the bolts must not only transmit the external load $2T$ but also the internal loads Q which develop due to the deflection of the flanges, as illustrated in figure 0.5.

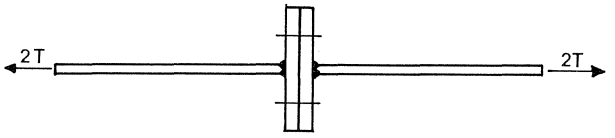

Fig. 0.3. T-stub connection.

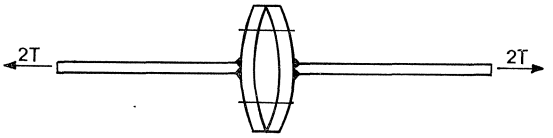

Fig. 0.4. Bending of the T-stub flange.

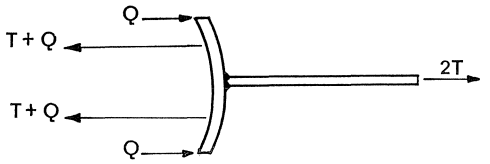

Fig. 0.5. Force distribution in the T-stub.

Contrary to the connection in figure 0.1, the planes (flange of the beam and web of the column) containing the tensile forces in figure 0.2 are perpendicular to each other.

This type of connections was usually avoided up till now because the deformations of the column flanges result in large deformations of the structure. Moreover, no design rules were available for this type of connections.

The deformations which occur on the tension side of a connection of the type shown in figure 0.2 are illustrated in figure 0.6.

These deformations will also cause internal loads Q to develop.

The position of these loads depends on the stiffness ratio between the T-stub and column flange.

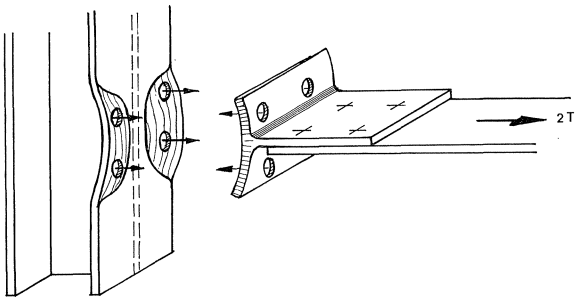

Fig. 0.6. Bending of the column flange and T-stub flange at the tension side of a moment connection.

The strength and the stiffness of the T-stub flange can be calculated when the dimensions are known.

However, a formula which allows the determination of the stiffness and strength of a column flange is lacking.

In this paper a theory is developed for the design of the tension side of statically loaded, bolted beam-to-column connections based on the plastic behaviour of the flanges and the bolts under the assumption that the plastification is large enough to allow the adoption of the most favourable static equilibrium.

In chapter 1 a method of design of T-stub connections is given which takes into account the internal loads Q (prying force).

A philosophy which shows that the design method of T-stubs can be applied also to connections corresponding to figure 0.2 is described in chapter 2. An important assumption in this philosophy is that the "effective" length of the column flange is known.

Chapter 3 describes the derivation of a formula for the effective length of a column flange in tension. This formula can be applied to bolted beam-to-column connections.

The derivation of the "effective" length formula is based on the analysis of two different collapse mechanisms.

Mechanism (1) occurs if bolt failure governs collapse. Mechanism (2) corresponds to collapse which results from failure of the flanges.

The derived formulas are in good agreement with test results even when the column flanges are stiffened with additional plates, parallel to the column flanges.

Twenty-eight specimens were tested in order to compare the maximum strength capacity of the connections with the calculated design values which follow from the theory developed in chapter 1, 2 and 3 (for test specimens see figures 0.3 and 0.7).

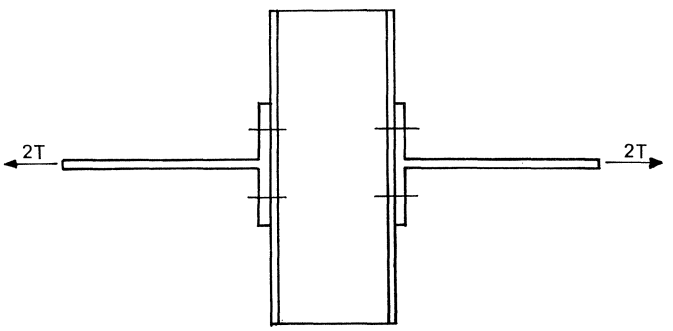

Fig. 0.7. Test specimen.

These tests are discussed in chapter 4.

Twenty-eight specimens of the type shown in figures 0.8 and 0.9 were used to verify that the developed design rules lead to connections which satisfy the limit states of deformations as given in the Dutch regulations for constructional steel work.

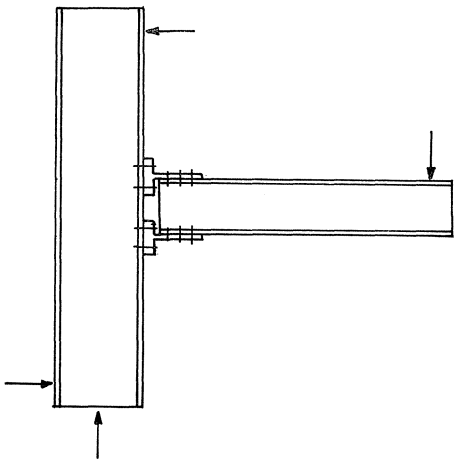

Fig. 0.8. Test specimen used to check the limit states of deformation.

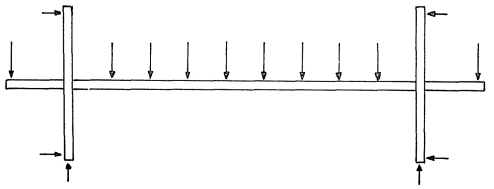

Fig. 0.9. Test specimen used to check the limit states of deformation given in the T.G.B. 1972-Staal.

These limit states of deformations are discussed in chapter 5 together with the conditions derived for beam-to-column connections.

The tests are discussed in chapter 6.

1 A design method for T-stub connections

1.1 *Introduction*

The theory of the design method is based on the plastic behaviour of the T-stub flanges and the bolts and on the assumption that the plastification is large enough to allow the adoption of the most favourable static equilibrium. Furthermore it is assumed that the plastic deformations in the flange plates and/or the bolts occur before failure of the structure itself. Simple plastic hinges are thought to form eventually at the bolt and the web line with bending moments equal to

$$M_p = \frac{bt^2\sigma_e}{4} \quad \text{and} \quad M'_p = \frac{bt^2\sigma_e}{4}$$

The collapse mechanisms which can form are subdivided into mechanism A (bolt failure is the determining factor) and mechanism B (the plastification of the flange plate is the determining factor).

The mechanisms are shown in figure 1.1.

In mechanism A, a prying force $Q < Q_{max}$ (including $Q = 0$) can be present at the end of the span n.

In mechanism B the prying force Q at the ends of the span n reaches its maximum value and causes a plastic hinge to form at the bolt line in the flange plate.

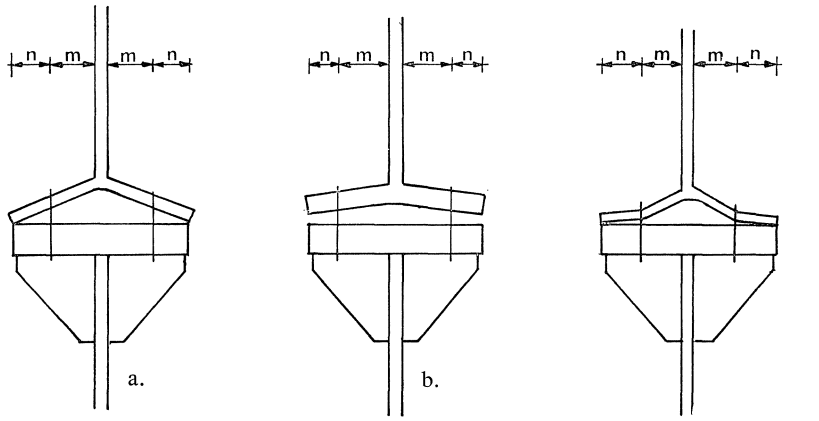

Collapse mechanism A

Collapse mechanism B

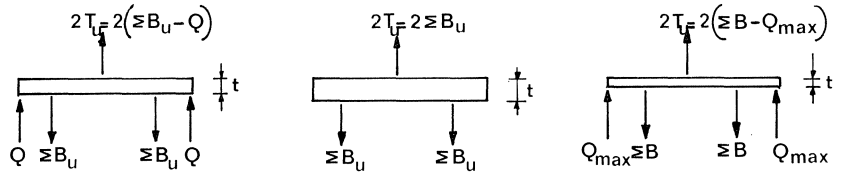

The forces on the plates

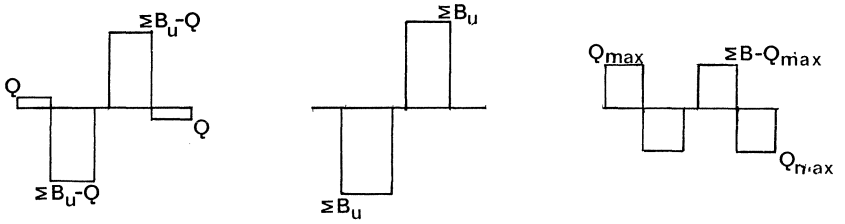

Shear force distribution

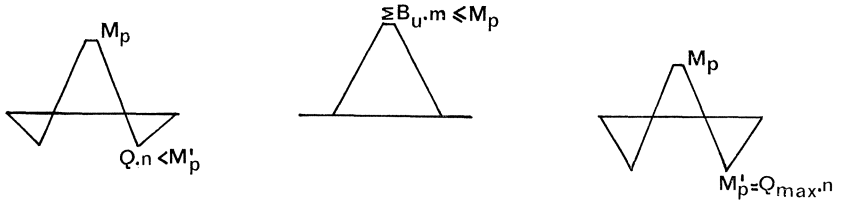

Moment distribution

Fig. 1.1. Simplified models of collapse mechanisms with prying forces.

The force distribution, moment distribution and shear force distribution corresponding to the two collapse mechanisms are given in figure 1.1.

where

ΣB_u* = the total ultimate tensile load of the bolts
ΣB = the total bolt force
T = the tensile load applied to one half of the construction
Q = the prying force between the flange plate and the support. It is assumed that this force acts on the ends of the span n
M_p = the plastic moment that causes a plastic hinge to form immediately adjacent to the tensile strip
M_p' = the plastic moment that causes a plastic hinge to form at the bolt line.

* Due to the symmetry of the connection only one half will be considered.

Remark

The influence of the shear forces on the plastic moment has been neglected.

1.2 *Collapse mechanism A* (the bolt fracture is the determining factor)

There are two possibilities.

a. A plastic hinge is formed next to the tensile strip before the ultimate tensile load of the bolt has been reached. At the end of the span n a force, Q, has developed, which decreases the ultimate tensile load T_u because $T_u = \Sigma B_u - Q$. There will either be no plastic hinge at the bolt line or this hinge will have been formed simultaneously with the rupture of the bolt.

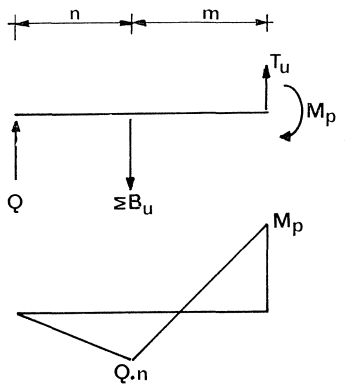

Fig. 1.2. Force distribution and moment distribution of collapse mechanism A, a.

T_u = the ultimate tensile load of one side of the connection
ΣB_u = the total ultimate tensile load of the bolts fitted at one side of the connection

$M_p = \frac{1}{4}bt^2\sigma_e$ is the plastic moment that causes a plastic hinge to form
b = the width of the flange plate
t = thickness of the flange plate
σ_e = yield stress.

Therefore, the following hold for collapse mechanism A:

$$\left.\begin{aligned} T_u &= \Sigma B_u - Q \\ T_u \times m - Q \times n &= M_p \end{aligned}\right\}$$ these two relations combined into one formula yield

$$T_u \times m - (\Sigma B_u - T_u) \times n = M_p \qquad (1\text{-}1)$$

b. The flange is heavy with respect to the rigidity of the bolt (figure 1.1 – collapse mechanism A, b).
There will either be no plastic hinge next to the tensile strip (web of the T-section) or this hinge will be formed simultaneously with the failure of the bolts, $Q = 0$. Therefore, for this mechanism, it holds that:

$$T_u \times m \leqslant M_p$$

which follows directly from (1-1), because

$$\Sigma B_u = T_u$$

These two formulas are already included in the formula (1-1) with $Q = 0$.

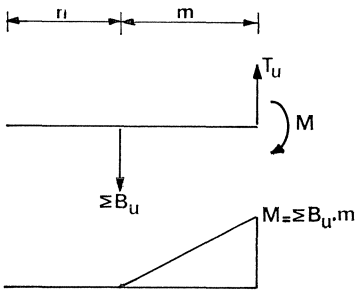

Fig. 1.3. Force distribution and the moment distribution of collapse mechanism A, b.

1.3 *Collapse mechanism B* (the flange plate is the determining factor)

If Q reaches its maximum value, then collapse mechanism B will come into being. The prying force Q reaches its maximum value when a plastic hinge is formed at the bolt line.

$$Q \times n = M'_p$$

$$Q_{\max} = \frac{M'_p}{n}$$

Now formula (1-1) changes to:

$$T_u \times m - \frac{M'_p}{n} \times n = M_p$$

$$T_u \times m = M_p + M'_p \tag{1-2}$$

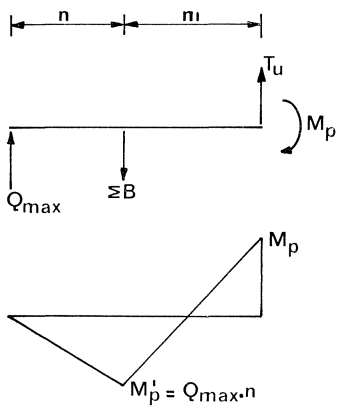

Fig. 1.4. Force distribution and moment distribution of collapse mechanism B.

In this case the flange plate is the determining factor. Now $T_u = \Sigma B - Q$, but ΣB will be equal to ΣB_u only in the optimum case.

ΣB is the bolt force immediately prior to the formation of a plastic hinge at the bolt line. In other words, increasing the bolt diameter yields a larger ΣB_u, but not a larger T_u.

Remarks

In summarizing, the next points are important. At constant T_u and increasing Q the ultimate tensile load of the bolts ΣB_u must also increase ($\Sigma B_u = T_u + Q$, a larger bolt diameter is necessary) as a result of which the flange plate thickness may decrease.

$$T_u \times m - Q \times n = M_p = \tfrac{1}{4} b t^2 \sigma_e$$

If $Q = 0$, then $T_u = \Sigma B_u$, but the flange plate thickness is determined by

$$T_u \times m = M_p$$

This gives the minimum allowable thickness of the flange plate using the smallest bolt at a given T.

If one takes

$$Q = Q_{\max} = \frac{M'_p}{n}$$

then $T_u \times m = M_p + M'_p = 2 \times \frac{1}{4} b t^2 \sigma_e$ from which the minimum required thickness of the flange plate may be computed for a given T using the largest bolt diameter.

The deformations immediately prior to collapse are the determining factors for the ultimate load of the connection.

With a heavy flange plate, for example, the deflection of the flange plate in the elastic stage might be larger than the elongation of the bolts.

In this stage a prying force can exist.

However, immediately prior to collapse, the elongation of the bolts is larger than the deflection of the flange-plate.

So, at that moment, there is no prying force and the bolt force is equal to the external load.

Assuming now that the adopted collapse mechanism at which $0 \leqslant Q \leqslant Q_{\max}$ really occurs (in other words the plastic behaviour of flange plate and bolt is such that the collapse mechanism adopts to this method of computation) then, adopting load factor design, the following two conditions must be satisfied:

$$T \times m - (\Sigma B_u - T)n \leqslant M_p \quad \text{where} \quad (\Sigma B_u - T) \geqslant 0 \quad \text{else} \quad T = \Sigma B_u \tag{1-3}$$

$$T \times m \leqslant M_p + M'_p \tag{1-4}$$

This means, in fact, that one is free to choose the desired collapse mechanism and consequently plate thicknesses and bolt diameters within certain limits.

1.4 *Adaptation to limit state design*

The objection to formulas (1-3) and (1-4) is that on the one hand one uses the *ultimate* load of the bolt and on the other hand the *plastic* moments of the plate in the design.

It would be more correct to include the yield strength of the bolt too. For the high-strength steel of the bolt it is not quite clear which strength should be taken.

The T.G.B. 1972–Staal (Dutch standards, Regulation for the calculation of building structures, Design of steel structures) has adopted limit state design.

The effects of the design loads (based on a load factor $\gamma = 1.5$) should be such that no limit state is exceeded. A limit state is defined as a condition where the structure ceases to function properly, for example due to large deformations. It can be said that the ultimate limit state of the T-stubs is reached when the mechanism with two plastic hinges comes into being. The T.G.B. 1972–Staal considers as the limit state of bolts in tension a tensile load equal to

$$\hat{F}_t = \sigma_e A_s$$

where

A_s = stress area of the bolt

σ_e = yield stress of the bolt material according to the standards.

when

$\sigma_e (\text{or } \sigma_{0.2}) > 0{,}7\sigma_t$ then $\sigma_e = 0{,}7\sigma_t$

σ_t = tensile stress of the bolt material.

The requirement $\sigma_e \leqslant 0{,}7\sigma_t$ is included to assure a sufficient margin of safety against bolt fracture.

With a load factor $\gamma = 1{,}5$, the safety factor against fracture of the bolts is at least $1{,}5/0{,}7 = 2{,}14$.

Formulas (1-3) and (1-4) are transformed into

$$T \cdot m - (\Sigma \hat{B}_t - T) \cdot n \leqslant M_p \quad \text{if} \quad (\Sigma \hat{B}_t - T) \geqslant 0 \quad \text{else} \quad T = \Sigma \hat{B}_t \tag{1-5}$$

if bolt fracture is the determining factor

$$T \cdot m \leqslant M_p + M'_p \tag{1-6}$$

if the flange plate is the determining factor

T = half of the design load

$\Sigma \hat{B}_t$ = the total limit load of the bolts fitted at one side of the T-stub connection.

The formulas (1-5) and (1-6) can be applied directly to connections where the strips introducing the tensile forces are in alignment. The plane of symmetry *a–a* shown in figure 1.5 can be considered as being rigid.

However, the situation for the bolts is not the same as with a rigid base because the bolts must now follow the deflections of two flange plates. Nevertheless the theory is directly applicable.

For connections in which the planes containing the tensile forces are perpendicular to each other (figure 0.7) the theory developed in this chapter can not be applied directly.

In the next chapter, however, a philosophy will be discussed which allows the use of formulas (1-5) and (1-6) for these connections also.

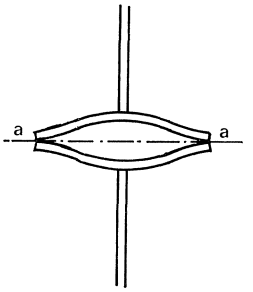

Fig. 1.5. The plane of symmetry a-a can be considered as rigid base.

2 A design method for T-stub flange to column connections

In a T-stub flange to column connection, the planes containing the tensile forces are perpendicular to each other. Separated prying forces, Q_1 (T-stub flange) and Q_2 (column flange), can not develop in this type of connections (figure 2.1).

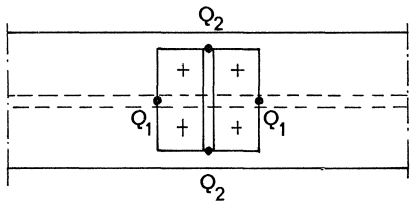

Fig. 2.1. Impossible position of the prying forces.

Figure 0.6 shows that the deflections prohibit this. However, a system of four symmetrical prying forces, each of magnitude $\frac{1}{2}Q$, does develop. Examples of the positions of these forces are shown in figures 2.2 and 2.3.

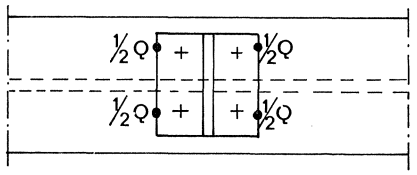

Fig. 2.2. Position of the prying forces when the T-stub flange has less rigidity than the column flange.

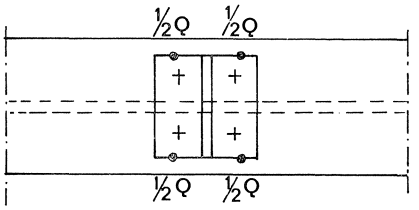

Fig. 2.3. Position of the prying forces when the T-stub flange is more rigid than the column flange.

The situation shown in figure 2.2 will occur if the T-stub flange has less rigidity than the column flange, while the situation illustrated in figure 2.3 will occur if the T-stub flange is more rigid than the column flange.

The optimum situation develops when the T-stub flange has the same rigidity as the column flange. Then the forces, $\frac{1}{2}Q$, develop at the corners of the T-stub flange (see figure 2.4).

This means that the T-stub flange as well as the column flange has the force distribution as given in figure 2.4.

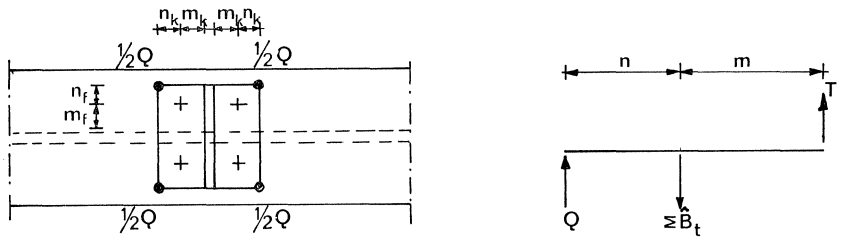

Fig. 2.4. Position of the prying forces when the T-stub flange and the column flange have the same rigidity (optimum situation).

The formulas applicable to both flange plates are:

$$T \cdot m - (\Sigma \hat{B}_t - T) \cdot n \leqslant M_p$$

$$(\Sigma \hat{B}_t - T) \geqslant 0 \quad \text{else} \quad T = \Sigma \hat{B}_t \tag{1-5}$$

$$T \cdot m \leqslant M_p + M'_p \tag{1-6}$$

Assume that the above-mentioned formulas give a higher value of T for the T-stub flange than for the column flange; in that case the column flange is the determining factor.

At the moment that the column flange reaches its optimum situation (failure at the highest obtainable T), the T-stub flange will not yet have reached its optimum.

This means that the forces $\frac{1}{2}Q$ given by the computation of the column flange are not in the position shown in figure 2.4 but in the position shown in figure 2.3; the stress in the T-stub flange has not yet reached the maximum value as will be evident from the following.

The T-stub flange is subjected to an actual force T smaller than the computed force T.

The optimum situation has been assumed, however, for the computation of the T-stub flange with

$$T \cdot m - (\Sigma \hat{B}_t - T) \cdot n = M_p \tag{2-1}$$

$$T \cdot m = M_p + M'_p \tag{2-2}$$

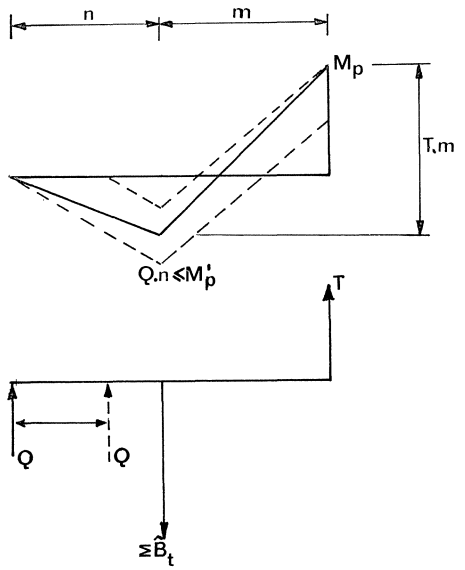

Fig. 2.5. Optimum design situation of the T-stub flange with possible moment distributions corresponding to smaller values of T resulting from failure of the column flange.

Assume now that formula (2-1) (mechanism A) governs. Then, mathematically speaking, to satisfy equation (2-1) with a smaller T, n has to be taken smaller in order to keep the right hand side of the equation constant and/or the right-hand side of equation (2-1) should be less than M_p.

Consequently, the stress must decrease.

The optimum design situation for the T-stub flange is shown in figure 2.5.

Possible moment distributions corresponding to smaller values of T resulting from failure of the column flange are shown as dotted lines.

These moment distributions are not important for the computation because it is assumed that the actual situation occurring in the T-stub flange will never be more adverse for the bolt or the plate than the optimum computed situation will be.

In other words, the construction adjusts itself to the situation and is in danger only if the smallest of the computed loads T is exceeded in the optimum.

The T-stub flange and the column flange can be computed separately with formulas (2-1) and (2-2) and the smallest value for the load T given by this computation is the design value.

It is necessary, however, to know the effective length of the column flange to be able to compute the proper value of the load.

Remarks

In the equilibrium situation it is assumed that the prying force $Q = \Sigma \hat{B}_t - T$ acts at the extreme edge of the plate.

Undoubtedly there are limits for the value of n, the extent of which has not yet been determined.

According to McGuire [2] the value n should be less than $n \leqq 1{,}25m$.

3 The effective length of the column flange

3.1 *Method of calculation*

In this chapter, a method of calculation for the column flange is derived which is identical to the method of calculation for the T-stub described in chapter 1.

With that in mind, tests have been performed. The testing of the specimens was continued until collapse mechanisms as shown in figure 3.1 were observed.

As with the T-stubs, two different collapse mechanisms are possible for the column flange; one occurs if bolt fracture is the determining factor, the other if the flange plate collapses.

The assumed collapse mechanisms I and II are given in figure 3.2. These theoretical mechanisms show a good resemblance with the mechanisms observed during the tests.

If simple plastic theory is applied, thus assuming that the elastic deformations are negligible, then mechanisms I and II are comparable with collapse mechanisms A and B of the T-stub flanges shown in figure 1.1. In mechanism I a prying force $Q < Q_{max}$ acts at the ends of the span n.

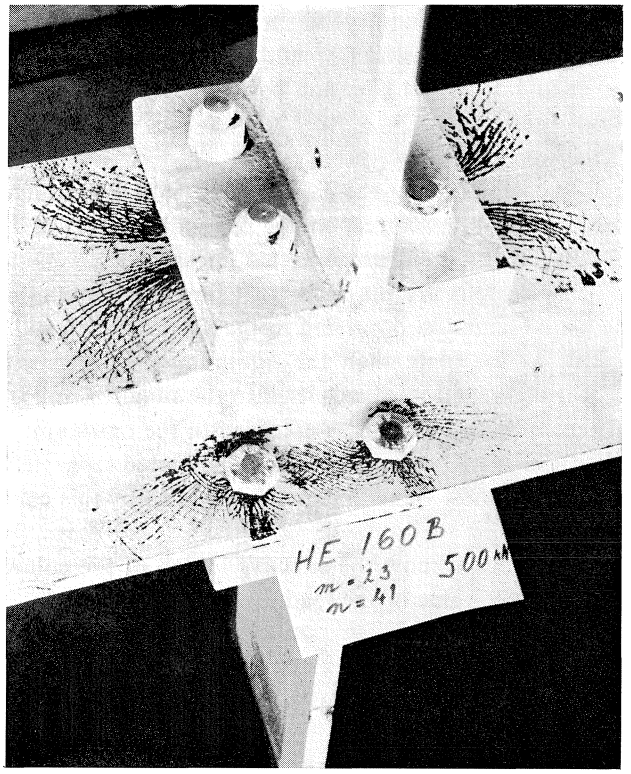

Fig. 3.1. Collapse mechanism of the column flange.

In mechanism II the prying force Q at the ends of the span n reaches the maximum value and causes a plastic hinge to form at the bolt lines in the flange plate.

The force moment and shear force distribution of the two collapse mechanisms bear a resemblance with the corresponding distributions of mechanisms A and B shown in figure 1.1. As an example, the moment distributions of figure 1.1 are also shown in figure 3.2. If M_p and M'_p in figure 3.2, can be determined by limit analysis of the collapse mechanisms, then the formulas

$$T \cdot m - (\Sigma \hat{B}_t - T)n \leqslant M_p \tag{1-5}$$

and

$$T \cdot m \leqslant M_p + M'_p \tag{1-6}$$

can be applied for these mechanisms too.

3.2 *Limit analysis of collapse mechanisms I and II*

3.2.1 Collapse mechanism I (bolt fracture is the determining factor)

The mode of collapse of the flange plate is shown in figure 3.3. Because of symmetry only one side is considered.

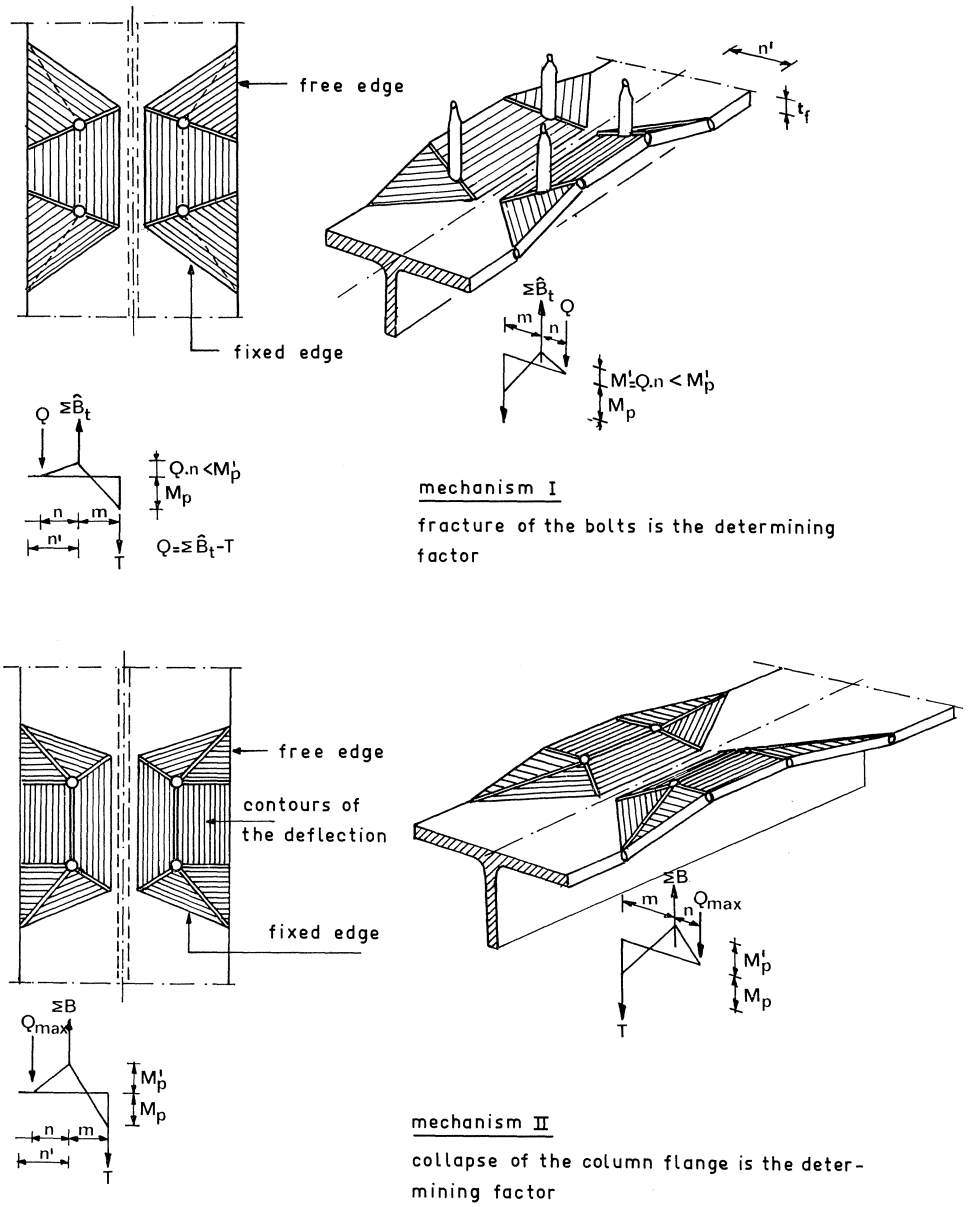

Fig. 3.2. Two collapse mechanisms of the column flanges in bolted beam-to-column connections. Notice the resemblance with the moment distributions as shown in figure 1.1.

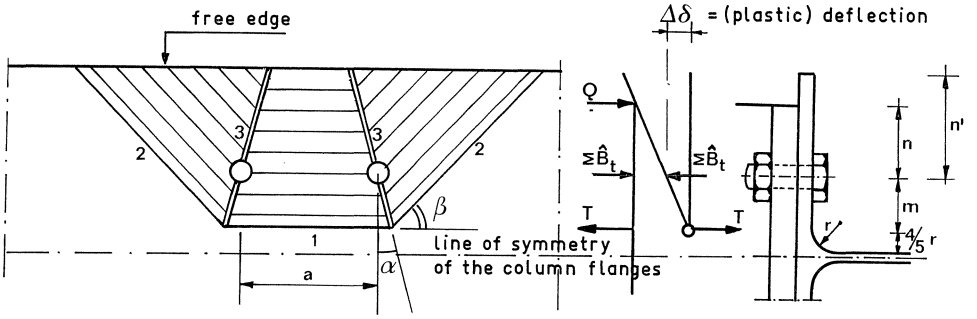

Fig. 3.3. Collapse mechanism I.

There are two unknowns in this figure, the angles α and β.

The problem is to minimize the collapse load for the total family of mechanisms, that is to say to find the values of α and β which give the smallest collapse load.

The internal dissipation of energy (ΔE) must be equal to the work done by the external loads (ΔT), neglecting the elastic energy.

$$\Delta E = \Delta T \tag{3-1}$$

Suppose that in figure 3.3 the center of the bolt holes are given a (plastic) deflection $\Delta\delta$ with respect to the line through the plastic hinge 1. Then the internal dissipation of energy can be calculated as follows:

Yield line 1 (see figure 3.3)

The length of this yield line is: $a+2m\cdot\mathrm{tg}\,\alpha$

The rotation is: $\dfrac{\Delta\delta}{m}$

Thus

$$\Delta E_1 = (a+2m\cdot\mathrm{tg}\,\alpha)\cdot\frac{\Delta\delta}{m}\cdot m_p,$$

where m_p is the yield moment per unit length of the plate.

Yield line 2 (see figure 3.3)

The length of this yield line is:

$$2\cdot\frac{m+n'}{\sin\beta}$$

The rotation is:

$$\frac{\Delta\delta}{\dfrac{m}{\cos\alpha}\cdot\cos(\beta-\alpha)}$$

Thus

$$\Delta E_2 = 2 \cdot \frac{m+n'}{\sin\beta} \frac{\cos\alpha}{\cos(\beta-\alpha)} \cdot \frac{\Delta\delta}{m} \cdot m_p$$

Yield line 3 (see figure 3.3)

The length of this yield line is:

$$2 \cdot \frac{m+n'}{\cos\alpha}$$

The rotation of yield line 3 follows from the rotation of yield line 1 and 2 as shown in the adjacent figure.

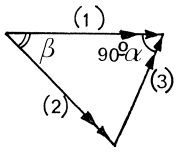

(1) = rotation of yield line 1
(2) = rotation of yield line 2
(3) = rotation of yield line 3

$$\frac{(3)}{\sin\beta} = \frac{\frac{\Delta\delta}{m}}{\sin(90°-\beta+\alpha)} \rightarrow (3) = \frac{\Delta\delta}{m} \cdot \frac{\sin\beta}{\cos(\beta-\alpha)}$$

Thus

$$\Delta E_3 = 2\frac{m+n'}{m} \frac{\sin\beta}{\cos(\beta-\alpha)\cdot\cos\alpha} \cdot \Delta\delta \cdot m_p$$

The contribution of the *bolt force* to the internal dissipation of energy can be calculated as follows.

The increase of the bolt length follows from the adjacent figure.

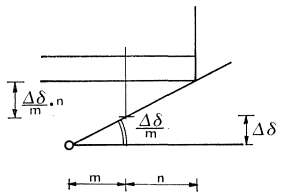

The increase of the bolt length due to a bolt force $\Sigma\hat{B}_t$ (the design strength) is

$$\frac{\Delta\delta}{m} \cdot n$$

Thus

$$\Delta E_4 = \Sigma\hat{B}_t \cdot \frac{\Delta\delta}{m} \cdot n$$

The total energy dissipated internally is:

$$\sum_{i=1}^{4} \Delta E_i = \left[\left\{ a + 2m \cdot \operatorname{tg}\alpha + 2(m+n') \frac{\cos\alpha}{\sin\beta \cdot \cos(\beta-\alpha)} + \right.\right.$$
$$\left.\left. + 2(m+n') \frac{\sin\beta}{\cos(\beta-\alpha) \cdot \cos\alpha} \right\} \cdot m_p + \Sigma \hat{B}_t \cdot n \right] \cdot \frac{\Delta\delta}{m} \tag{3-2}$$

The force Q causes only elastic deformations and therefore does not contribute to the internal energy dissipation.

The work done by the external force T is equal to

$$\Delta T = T \cdot \frac{m+n}{m} \cdot \Delta\delta \tag{3-3}$$

From equations (3-1), (3-2) and (3-3) it follows that

$$T \cdot (m+n) = \left\{ a + 2m \cdot \operatorname{tg}\alpha + 2 \cdot (m+n') \frac{\cos\alpha}{\sin\beta \cdot \cos(\beta-\alpha)} + \right.$$
$$\left. + 2 \cdot (m+n') \frac{\sin\beta}{\cos(\beta-\alpha) \cdot \cos\alpha} \right\} m_p + \Sigma \hat{B}_t \cdot n =$$
$$= \left\{ a + 2m \cdot \operatorname{tg}\alpha + 2(m+n') \frac{\cos^2\alpha + \sin^2\beta}{\cos\alpha \cdot \sin\beta \cdot \cos(\beta-\alpha)} \right\} \cdot m_p + \Sigma \hat{B}_t \cdot n \tag{3-4}$$

It appears from equation (3-4) that minimizing the load T implies minimizing the right hand side of the equation because $(m+n)$ is a constant.

It is evident that in order to find a minimum collapse load, the following conditions must be satisfied:

$$\frac{\partial \sum_{i=1}^{4} \Delta E_i}{\partial\alpha} = 0 \tag{3-5}$$

and

$$\frac{\partial \sum_{i=1}^{4} \Delta E_i}{\partial\beta} = 0 \tag{3-6}$$

Carrying out the differentiation:

$$\frac{m}{\Delta\delta \cdot m_p} \frac{\partial \sum_{i=1}^{4} \Delta E_i}{\partial\alpha} = \frac{2m}{\cos^2\alpha} + 2(m+n') \left[\frac{2\cos\alpha \cdot -\sin\alpha \cdot \cos\alpha \cdot \sin\beta \cdot \cos(\beta-\alpha)}{\cos^2\alpha \cdot \sin^2\beta \cdot \cos^2(\beta-\alpha)} - \right.$$

$$-(\cos^2\alpha+\sin^2\beta)\cdot\left\{\frac{-\sin\alpha\cdot\sin\beta\cdot\cos(\beta-\alpha)-\cos\alpha\cdot\sin\beta\cdot\sin(\beta-\alpha)\cdot-1}{\cos^2\alpha\cdot\sin^2\beta\cdot\cos^2(\beta-\alpha)}\right\}\Bigg]=$$

$$=\frac{2m\cdot\cos^2(\beta-\alpha)-2(m+n')\{-\cos^2\alpha(\sin^2\alpha+\cos^2\alpha)+2\sin\alpha\cdot\cos\alpha\cdot\sin\beta\cdot\cos\beta\}}{\cos^2\alpha\cdot\cos^2(\beta-\alpha)}+$$

$$+\frac{-2(m+n')(\sin^2\alpha-\cos^2\alpha)\sin^2\beta}{\cos^2\alpha\cdot\cos^2(\beta-\alpha)}=$$

$$=2m\cdot\frac{\cos^2(\beta-\alpha)-\dfrac{m+n'}{m}\{\sin^2(\alpha-\beta)+\cos 2\alpha\}}{\cos^2\alpha\cdot\cos^2(\beta-\alpha)}=0 \qquad (3\text{-}7)$$

$$\frac{m}{\Delta\delta\cdot m_p}\frac{\partial\sum_{i=1}^{4}\Delta E_i}{\partial\beta}=2(m+n')\left[\frac{2\sin\beta\cdot\cos\beta\cdot\cos\alpha\cdot\sin\beta\cdot\cos(\beta-\alpha)}{\cos^2\alpha\cdot\sin^2\beta\cdot\cos^2(\beta-\alpha)}-\right.$$

$$\left.-\frac{(\cos^2\alpha+\sin^2\beta)\cdot\cos\alpha\cdot\cos\beta\cdot\cos(\beta-\alpha)-\sin\beta\cdot\sin(\beta-\alpha)}{\cos^2\alpha\cdot\sin^2\beta\cdot\cos^2(\beta-\alpha)}\right]=$$

$$=2(m+n')\frac{\sin^2\beta\cdot\cos\{\beta-(\beta-\alpha)\}-\cos^2\alpha\cdot\cos\{\beta+(\beta-\alpha)\}}{\cos\alpha\cdot\sin^2\beta\cdot\cos^2(\beta-\alpha)}=$$

$$=2(m+n')\frac{\sin^2\beta\cdot\cos\alpha-\cos^2\alpha\cdot\cos(2\beta-\alpha)}{\cos\alpha\cdot\sin^2\beta\cdot\cos^2(\beta-\alpha)}=0 \qquad (3\text{-}8)$$

In figure 3.3 it can be seen that

$$\cos^2\alpha\cdot\cos^2(\beta-\alpha)\neq 0 \quad \text{and} \quad \cos\alpha\cdot\sin^2\beta\cdot\cos^2(\beta-\alpha)\neq 0$$

will always be satisfied, then equation (3-7) can be reduced to

$$\cos^2(\beta-\alpha)=\frac{m+n'}{n}\{\sin^2(\alpha-\beta)+\cos 2\alpha\} \qquad (3\text{-}9)$$

and equation (3-8) can be reduced to

$$\sin^2\beta=\cos\alpha\cdot\cos(2\beta-\alpha)=\cos\alpha\cdot\cos 2\beta\cdot\cos\alpha+\cos\alpha\cdot\sin\beta\cdot\sin\alpha$$

$$\tfrac{1}{2}(1-\cos 2\beta)=\cos^2\alpha\cdot\cos 2\beta+\cos\alpha\cdot\sin\alpha\cdot\sin 2\beta$$

$$\tfrac{1}{2}=(\cos^2\alpha+\tfrac{1}{2})\cos 2\beta+\tfrac{1}{2}\sin 2\alpha\cdot\sin 2\beta$$

$$\tfrac{1}{2}=\tfrac{1}{2}\cos 2\beta+\tfrac{1}{2}\cos 2\beta+\tfrac{1}{2}\cos 2\alpha\cdot\cos 2\beta+\tfrac{1}{2}\sin 2\alpha\cdot\sin 2\beta$$

$$1=2\cos 2\beta+\cos 2(\alpha-\beta)$$

$$\cos 2(\alpha-\beta)+2\cos 2\beta-1=0$$

$$1-2\sin^2(\alpha-\beta)+2\cos 2\beta-1=0$$

$$\sin^2(\alpha-\beta)=\cos 2\beta \tag{3-10}$$

Substituting eq (3-10) into eq. (3-9) yields

$$\cos^2(\beta-\alpha)=\frac{m+n'}{m}\{\cos 2\beta+\cos 2\alpha\}=2\frac{m+n'}{m}\cos(\alpha+\beta)\cdot\cos(\alpha-\beta)$$

Thus

$$\cos(\beta-\alpha)=2\frac{m+n'}{m}\cos(\alpha+\beta) \tag{3-11}$$

Rewriting (3-11) gives

$$\operatorname{ctg}\beta=\frac{3m+2n'}{m+2n'}\operatorname{tg}\alpha \tag{3-12}$$

If the result of equation (3-12) is substituted into the numerator of equation (3-8) and after some simplification the following result is obtained:

$$\operatorname{tg}\alpha=\frac{m+2n'}{\sqrt{7m^2+12mn'+4n'^{2'}}} \tag{3-13}$$

By substituting eq. (3-13) into (3-12), β also can be expressed as a function of m and n'. If equation (3-4) is rewritten as a function of $\operatorname{tg}\alpha$ only, equation (3-14) is obtained.

$$T\cdot(m+n)=\left\{a+2m\cdot\operatorname{tg}\alpha+2(m+n')\cdot\frac{2+(1+q^2)\operatorname{tg}^2\alpha}{(1+q)\operatorname{tg}\alpha}\right\}m_p+\Sigma\hat{B}_t\cdot n \tag{3-14}$$

where

$$q=\frac{3m+2n'}{m+2n'}$$

If the value of $\operatorname{tg}\alpha$ as expressed in equation (3-13) is substituted into equation (3-14) it can be shown that equation (3-14) can be written as

$$T\cdot(m+n)=\{a+2\sqrt{7m^2+12mn'+4n'^{2'}}\}\cdot m_p+\Sigma\hat{B}_t\cdot n \tag{3-15}$$

Figure 3.4 shows that for practical ratios of m and n' $2\sqrt{7m^2+12mn'+4n'^2}$ can be replaced by $5{,}5m+4n'$. The resulting differences are given in percentages.

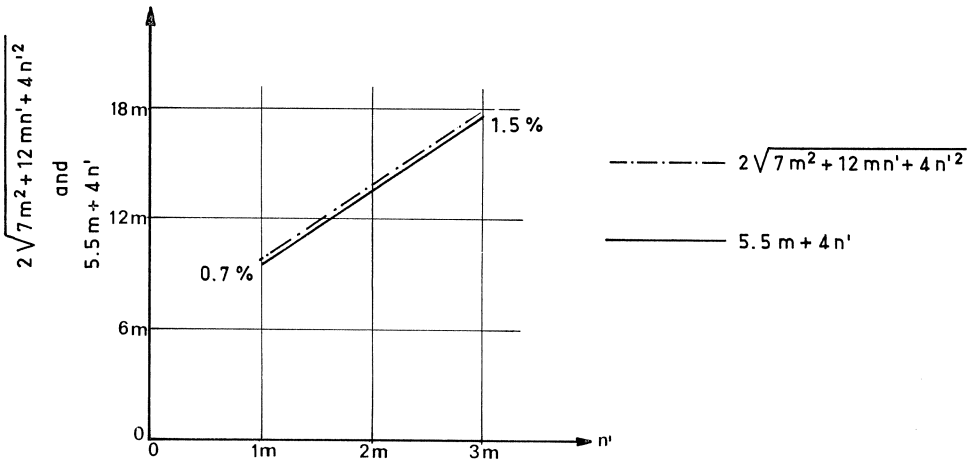

Fig. 3.4. Differences between $2\sqrt{7m^2+12mn'+4n'^2}$ and $5{,}5m+4n'$ for practical ratios of m and n'.

Therefore equation (3-15) can be transformed into

$$T\cdot m-(\Sigma\hat{B}_t-T)\cdot n=(a+5{,}5m+4n')\cdot m_p \tag{3-16}$$

where m_p is the yield moment per unit length of the plate.

From formula (1-5) $(T\cdot m-(\Sigma\hat{B}_t-T)\cdot n\leqslant M_p)$ and formula (3-16) it follows that for collapse mechanism I of a column flange M_p is equal to $(a+5{,}5m+4n')\cdot m_p$.

Hence, the length $(a+5{,}5m+4n')$ of a column flange is comparable with the width of a T-stub flange when collapse mechanism I is the mode of failure. Therefore $(a+5{,}5m+4n')$ can be considered as an effective length of the column flange. Because the elastic energy due to the force Q is neglected, formula (3-16) includes a great number of situations where Q varies between zero and Q_{max}.

The determination of the effective length of a column flange in tension as carried out above corresponds best to the situation where $Q=0$ then $\Sigma\hat{B}_t=T$, hence $T\cdot m=(a+5{,}5m+4n')\cdot m_p$.

The other situation where the prying force Q reaches its maximum value just prior to the formation of a plastic hinge at the bolt line can produce another effective length, as will be shown by a limit analysis of collapse mechanism II.

3.2.2 Collapse mechanism II (collapse of the column flange is the determining factor)

For a mechanism II failure, the prying force Q reaches its maximum value and causes the formation of a plastic hinge at the bolt line.

The mode of collapse of the flange plate is shown in figure 3.5. For reason of symmetry only one side is considered.

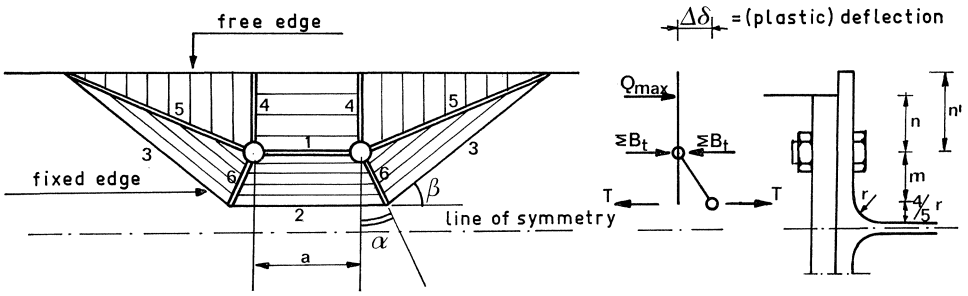

Fig. 3.5. Collapse mechanism II.

Again the unknowns in this figure are the angles α and β. The values of α and β which produce the smallest collapse load are of interest.

The same procedure as used in paragraph 3.2.1 will solve this problem. The work done by the external load T is equal to

$$\Delta T = T \cdot \Delta\delta \tag{3-17}$$

if it is supposed that the centers of the bolt holes are given a (plastic) deflection $\Delta\delta$.

The internal dissipation of energy is calculated as follows:

Yield line 1 (see figure 3.5)

The length of this yield line is: a

The rotation is: $\dfrac{\Delta\delta}{m}$

Thus:

$$\Delta E_1 = a \cdot \frac{\Delta\delta}{m} \cdot m_p,$$

where m_p is the yield moment per unit length of the plate.

Yield line 2 (see figure 3.5)

The length of this line is: $a + 2m \cdot \mathrm{tg}$

The rotation is: $\dfrac{\Delta\delta}{m}$

Thus:

$$\Delta E_2 = (a + 2m \cdot \mathrm{tg}\,\alpha) \cdot \frac{\Delta\delta}{m} \cdot m_p$$

Yield line 3 (see figure 3.5)

The length of this yield line is:

$$2 \cdot \frac{m + n'}{\sin\beta}$$

The rotation is

$$\frac{\Delta\delta}{\frac{m}{\cos\alpha}\cdot\cos(\beta-\alpha)}$$

Thus:

$$\Delta E_3 = 2\frac{m+n'}{\sin\beta}\cdot\frac{\cos\alpha}{\cos(\beta-\alpha)}\cdot\frac{\Delta\delta}{m}\cdot m_p$$

Yield line 4 (see figure 3.5)

The length of this yield line is: $2n'$
The rotation is $\Delta\delta/b$, where b is given in the adjacent figure.

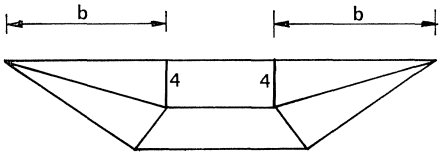

Thus:

$$\Delta E_4 = 2\cdot\frac{n'}{b}\cdot\Delta\delta\cdot m_p$$

Yield line 5 (see figure 3.5)

The length of this yield line is: $2\sqrt{b^2+n'^2} = 2l$
The calculation of the rotation follows from the adjacent figures.

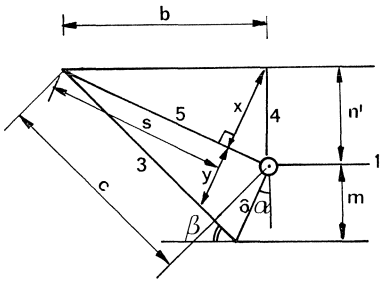

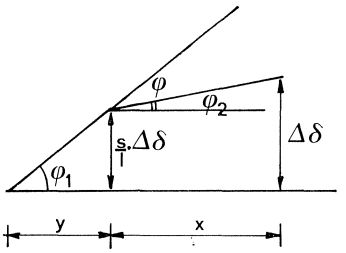

$$\varphi = \varphi_1 - \varphi_2 = \frac{\frac{s}{l}\Delta\delta}{y} - \frac{\Delta\delta - \frac{s}{l}\Delta\delta}{x} = \left(\frac{s}{ly} + \frac{s}{lx} - \frac{1}{x}\right)\cdot\Delta\delta$$

$$\Delta E_5 = 2l\cdot\varphi\cdot m_p = 2\cdot\left(\frac{s}{y} + \frac{s}{x} - \frac{l}{x}\right)\cdot\Delta\delta\cdot m_p$$

$$\frac{s}{y} = \frac{c}{\frac{m}{\cos\alpha}\cos(\beta-\alpha)} \qquad \frac{s}{x} = \frac{b}{n'}$$

$$\frac{x}{b} = \frac{n'}{l} \rightarrow x = \frac{bn'}{l} \rightarrow \frac{l}{x} = \frac{l^2}{bn'}$$

Hence:

$$\Delta E_5 = 2 \cdot \left\{ \frac{c \cdot \cos\alpha}{m \cdot \cos(\beta - \alpha)} + \frac{b}{n'} - \frac{l^2}{bn'} \right\} \cdot \Delta\delta \cdot m_p =$$

$$= 2 \left\{ \frac{c \cdot \cos\alpha}{m \cdot \cos(\beta - \alpha)} - \frac{n'}{b} \right\} \cdot \Delta\delta \cdot m_p$$

$$c = \left\{ \frac{c}{\cos\alpha} \cdot \cos(\beta - \alpha) + \frac{n'}{\cos\beta} \right\} \cdot \operatorname{ctg}\beta$$

Thus:

$$\Delta E_5 = 2 \left\{ \operatorname{ctg}\beta + \frac{n'}{m} \frac{\cos\alpha}{\sin\beta \cdot \cos(\beta - \alpha)} - \frac{n'}{b} \right\} \cdot \Delta\delta \cdot m_p$$

Yield line 6 (see figure 3.5)

The length of this yield line is: $2m/\cos\alpha$

The rotation of yield line 6 follows from the rotations of yield lines 2 and 3 as shown in the adjacent figure:

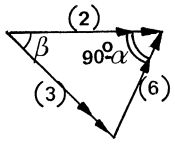

(2) = rotation of yield line 2
(3) = rotation of yield line 3
(6) = rotation of yield line 6

$$\frac{(3)}{\sin(90° - \alpha)} = \frac{(6)}{\sin\beta} \rightarrow (6) = \frac{\Delta\delta}{m} \cdot \frac{\sin\beta}{\cos(\beta - \alpha)}$$

Thus:

$$\Delta E_6 = 2 \cdot \frac{m}{\cos\alpha} \cdot \frac{\Delta\delta}{m} \cdot \frac{\sin\beta}{\cos(\beta - \alpha)} \cdot m_p$$

The bolts are subjected only to elastic deformations and do not contribute to the internal dissipation of energy.

The total internal energy will be:

$$\sum_{i=1}^{6} \Delta E_i = 2 \left\{ \frac{a}{m} + \operatorname{tg}\alpha + \frac{m + n'}{m} \cdot \frac{\cos\alpha}{\sin\beta \cdot \cos(\beta - \alpha)} + \frac{n'}{b} + \operatorname{ctg}\beta + \frac{n'}{m} \frac{\cos\alpha}{\sin\beta \cdot \cos(\beta - \alpha)} - \right.$$

$$\left. - \frac{n'}{b} + \frac{\sin\beta}{\cos\alpha \cdot \cos(\beta - \alpha)} \right\} \cdot \Delta\delta \cdot m_p$$

$$\sum_{i=1}^{6} \Delta E_i = 2 \left\{ \frac{a}{m} + \frac{m + 2n'}{m} \frac{\cos\alpha}{\sin\beta \cdot \cos(\beta - \alpha)} + \operatorname{tg}\alpha + \operatorname{ctg}\beta + \frac{\sin\beta}{\cos\alpha \cdot \cos(\beta - \alpha)} \right\} \Delta\delta \cdot m_p \tag{3-18}$$

Equating the internal and external energy gives:

$$T\cdot\Delta\delta = 2\left\{\frac{a}{m}+\frac{m+2n'}{m}\,\frac{\cos\alpha}{\sin\beta\cdot\cos(\beta-\alpha)}+\operatorname{tg}\alpha+\operatorname{ctg}\beta+\frac{\sin\beta}{\cos\alpha\cdot\cos(\beta-\alpha)}\right\}\cdot\Delta\delta\cdot m_p \tag{3-19}$$

As can be seen minimizing the load T implies minimizing the right hand side of the equation (3-19). It is evident that in order to find a minimum collapse load, the following conditions must be satisfied:

$$\frac{\partial\sum_{i=1}^{6}\Delta E_i}{\partial\alpha}=0 \tag{3-20}$$

$$\frac{\partial\sum_{i=1}^{6}\Delta E_i}{\partial\beta}=0 \tag{3-21}$$

Carrying out the differentiation:

$$\frac{1}{\Delta\delta\cdot m_p}\cdot\frac{\partial\sum_{i=1}^{6}\Delta E_i}{\partial\alpha}=\frac{m+2n'}{m}\cdot\frac{-\sin\alpha\cdot\sin\beta\cdot\cos(\beta-\alpha)-\cos\alpha\cdot\sin\beta\cdot-\sin(\beta-\alpha)\cdot-1}{\sin^2\beta\cdot\cos^2(\beta-\alpha)}+$$

$$+\frac{1}{\cos^2\alpha}+\sin\beta\cdot\frac{-1}{\cos^2\alpha\cdot\cos^2(\beta-\alpha)}\cdot\{-\sin\alpha\cdot\cos(\beta-\alpha)-\cos\alpha\cdot\sin(\beta-\alpha)\cdot-1\}=$$

$$=\frac{m+2n'}{m}\cdot\frac{-\sin^2\beta(\sin^2\alpha+\cos^2\alpha)}{\sin^2\beta\cos^2(\beta-\alpha)}+\frac{1}{\cos^2\alpha}+$$

$$+\frac{2\sin\alpha\cdot\cos\alpha\cdot\sin\beta\cdot\cos\beta+\sin^2\beta(\sin^2\alpha-\cos^2\alpha)}{\cos^2\alpha\cos^2(\beta-\alpha)}=$$

$$=-\frac{m+2n'}{m}\,\frac{1}{\cos^2(\beta-\alpha)}+\frac{1}{\cos^2\alpha}+\frac{\frac{1}{2}\sin2\alpha\cdot\sin2\beta+\sin^2\beta\cdot-\cos2\alpha}{\cos^2\alpha\cos^2(\beta-\alpha)}=$$

$$=-\frac{m+2n'}{m}\,\frac{1}{\cos^2(\beta-\alpha)}+\frac{\frac{1}{2}+\frac{1}{2}\cos2(\beta-\alpha)+\frac{1}{2}\cos(2\alpha-2\beta)-\frac{1}{2}\cos2\alpha}{\cos^2\alpha\cos^2(\beta-\alpha)}=0$$

Thus:

$$\frac{1}{\Delta\delta\cdot m_p}\cdot\frac{\partial\sum_{i=1}^{6}\Delta E_i}{\partial\alpha}=-\frac{m+2n'}{m}\,\frac{1}{\cos^2(\beta-\alpha)}+\frac{\cos2(\beta-\alpha)+\sin^2\alpha}{\cos^2\alpha\cdot\cos^2(\beta-\alpha)}=0 \tag{3-22}$$

$$\frac{1}{\Delta\delta\cdot m_p}\cdot\frac{\partial\sum_{i=1}^{6}\Delta E_i}{\partial\beta}=\frac{m+2n'}{m}\cdot\cos\alpha\cdot\frac{-1}{\sin^2\beta\cos^2(\beta-\alpha)}\cdot\{\cos\beta\cdot\cos(\beta-\alpha)+$$

$$+\sin\beta\cdot-\sin(\beta-\alpha)\}-\frac{1}{\sin^2\beta}+\frac{\cos\beta\cdot\cos\alpha\cdot\cos(\beta-\alpha)-\sin\beta\cdot\cos\alpha\cdot-\sin(\beta-\alpha)}{\cos^2\alpha\cdot\cos^2(\beta-\alpha)}=$$

$$=\frac{m+2n'}{m}\cdot\frac{\cos^2\alpha(\sin^2\beta-\cos^2\beta)-2\sin\alpha\cdot\cos\alpha\cdot\sin\beta\cdot\cos\beta}{\sin^2\beta\cdot\cos^2(\beta-\alpha)}-\frac{1}{\sin^2\beta}+$$

$$+\frac{\cos^2\alpha(\cos^2\beta+\sin^2\beta)}{\cos^2\alpha\cdot\cos^2(\beta-\alpha)}=$$

$$=\frac{m+2n'}{m}\cdot\frac{\sin^2\beta-\cos^2(\beta-\alpha)}{\sin^2\beta\cdot\cos^2(\beta-\alpha)}+\frac{\sin^2\beta-\cos^2(\beta-\alpha)}{\sin^2\beta\cdot\cos^2(\beta-\alpha)}=0$$

and

$$\frac{1}{\Delta\delta\cdot m_p}\cdot\frac{\partial\sum_{i=1}^{6}\Delta E_i}{\partial\beta}=\frac{2m+2n'}{m}\frac{\sin^2\beta-\cos^2(\beta-\alpha)}{\sin^2\beta\cdot\cos^2(\beta-\alpha)}=0 \tag{3-23}$$

In figure 3.5 it can be seen that

$$\cos^2\alpha\cdot\cos^2(\beta-\alpha)\neq 0 \quad\text{and}\quad \sin^2\beta\cdot\cos^2(\beta-\alpha)\neq 0$$

will always be satisfied.

Then, from eq. (3-23) it follows that:

$$\sin^2\beta=\cos^2(\beta-\alpha)\rightarrow\sin\beta=\cos\beta\cdot\cos\alpha+\sin\beta\cdot\sin\alpha \tag{3-24}$$

and from eq. (3-22):

$$\frac{m+2n'}{m}=\frac{\cos 2(\beta-\alpha)+\sin^2\alpha}{\cos^2\alpha}=\frac{2\sin^2\beta-\cos^2\alpha}{\cos^2\alpha}=\frac{2\sin^2\beta}{\cos^2\alpha}-1$$

$$\frac{m+n'}{m}=\frac{\sin^2\beta}{\cos^2\alpha}\rightarrow\cos\alpha=\frac{\sin\beta}{\sqrt{\frac{m+n'}{m}}} \tag{3-25}$$

Substituting eq. (3-25) into eq. (3-24) yields:

$$\sin\beta\left(1-\sqrt{1-\frac{\sin^2\beta}{\frac{m+n'}{m}}}\right)=\cos\beta\cdot\frac{\sin\beta}{\sqrt{\frac{m+n'}{m}}}$$

$$\cos\beta = \frac{1}{2\sqrt{\frac{m+n'}{m}}} \tag{3-26}$$

Now all the unknowns of the energy equation can be calculated.

When it is done and if the results are substituted into the energy equation the following relationship is found.

$$T\cdot\Delta\delta = 2\cdot\left(\frac{a}{m} + \frac{6m+8n'}{\sqrt{3m^2+4n'm}}\right)\cdot m_p\cdot\Delta\delta$$

and

$$T\cdot m = 2\left(a + \frac{6m+8n'}{\sqrt{3+\frac{4n'}{m}}}\right) m_p \tag{3-27}$$

Figure 3.6 shows that equation (3-27) can be approximated by

$$T\cdot m = 2(a+4m+1{,}25n')\cdot m_p \tag{3-28}$$

For practical m and n' ratios the differences between

$4m+1{,}25n'$ and $\dfrac{6m+8n'}{\sqrt{3+\frac{4n'}{m}}}$ are given in figure 3.6

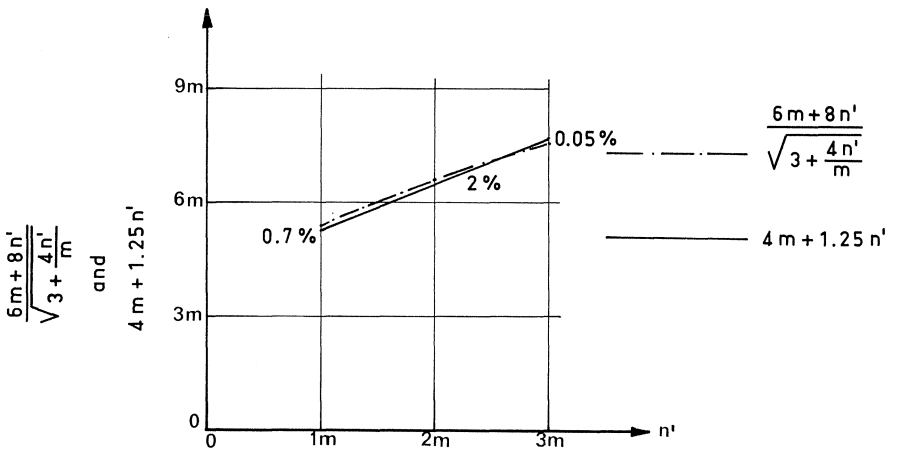

Fig. 3.6. Differences between $\dfrac{6m+8n'}{\sqrt{3+\frac{4n'}{m}}}$ and $4m+1{,}25n'$ for practical ratios of m and n'.

3.2.3 The effective length

It follows from the above formula (3-28) that for collapse mechanism II of a column flange the sum M_p+M_p' of formula (1-6) $T\cdot m \leqslant M_p+M_p'$ is equal to $2\cdot(a+4m+1{,}25n')m_p$.

The contribution of M_p' to the total moment is caused by the prying force Q. It is interesting to know the magnitude of M_p' because then an estimate of the value of M_p is obtained for Q varying between

$$Q=0 \quad \text{and} \quad Q=Q_{\max}=\frac{M_p'}{n}$$

for collapse mechanism I.

The influence of Q on the total yield moment of collapse mechanism II will be determined by an equilibrium analysis of that part of the column flange bounded by yield lines 1 and 5 and the free edge of the plate. It is assumed that yield lines 1 and 5 do not transmit torsional moments and shear forces.

Then moment equilibrium requires that

$$Q\cdot n = m_p\cdot a+2m_p\cdot b \text{ (see figure 3.7)} \tag{3-29}$$

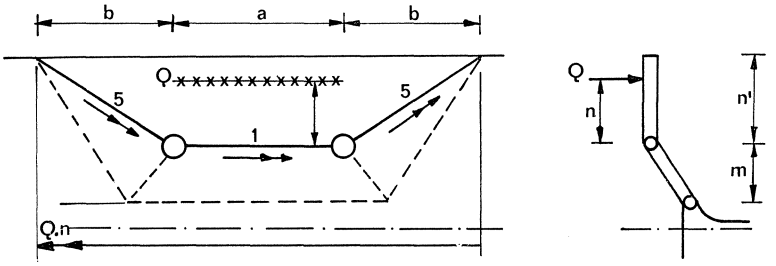

Fig. 3.7. Moment equilibrium of a part of the column flange.

It is already known that

$$b = m\cdot\operatorname{tg}\alpha+\frac{m+n'}{\sin\beta}=m\cdot\frac{m+2n'}{\sqrt{3m^2+4n'm}}+(m+n')\frac{2\sqrt{m+n'}}{\sqrt{3m+4n'}}=$$

$$=\frac{m^2+2mn'+(m+n')2\cdot\sqrt{m^2+mn'}}{\sqrt{3m^2+4n'm}}$$

Thus

$$Q_{\max}\cdot n=\left\{a+2\cdot\frac{m^2+2mn'+(m+n')2\sqrt{m^2+mn'}}{\sqrt{3m^3+4n'm}}\right\}\cdot m_p \tag{3-30}$$

This equation can be approximated by

$$Q_{\max}\cdot n=(a+4m+2{,}5n')\cdot m_p \tag{3-31}$$

as shown in figure 3.8 where the difference between

$$2 \cdot \frac{m^2 + 2mn' + (m+n')2\sqrt{m^2+mn'}}{\sqrt{3m^2+4n'm}}$$

and $4m+2{,}5n'$ is given for practical ratios of m and n'.

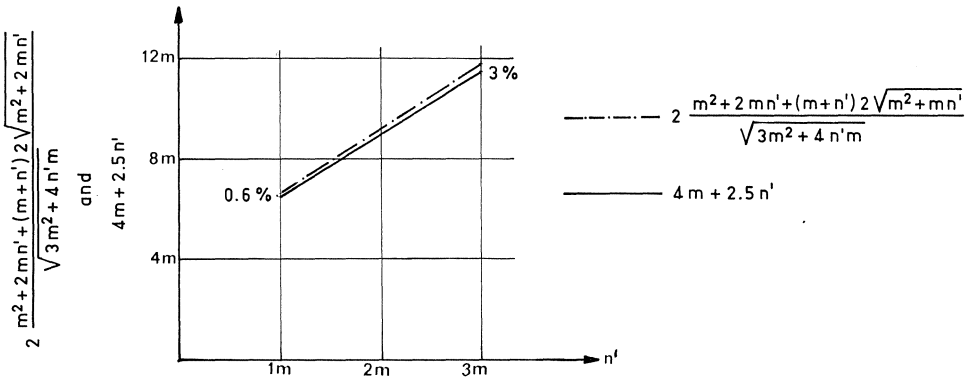

Fig. 3.8. Differences between 2. $\frac{m^2+2m'+(m+n')2\sqrt{m^2+2mn'}}{\sqrt{3m^2+4n'm}}$ and $4+2{,}5n'$ for practical ratios of m and n'.

From formula (1-6)

$$T \cdot m \leqslant M_p + M_p';$$

eq. (3-28)

$$T \cdot m = 2(a+4m+1{,}25n') \cdot m_p$$

and eq. (3-39)

$$Q_{\max} \cdot n = (a+4m+2{,}5n') \cdot m_p$$

it follows that M_p is equal to $(a+4m) \cdot m_p$ for collapse mechanism II.

It appears from this obtained value of M_p and from the value determined with collapse mechanism I that the effective length of the column flange which determines the magnitude of M_p depends on the value of the prying force Q.

The foregoing analysis yields the boundary values between which M_p varies when Q varies between $Q = 0$ and $Q = Q_{\max}$

for $Q = 0$ $\quad M_p = (a+5{,}5m+4n') \cdot m_p$ (see page 25)

for $Q = Q_{\max}$ $\quad M_p = (a+4m) \cdot m_p$

Now a decision must be made about the value of *the effective length* which should be adopted for design purposes.

If $M_p = (a+5{,}5m+4n')\cdot m_p$ is chosen, then the safety factor against bolt failure is too small if Q should approach its maximum value.

If $M_p = (a+4m)\cdot m_p$ is chosen then the safety factor against bolt failure is too large in the situation where $Q = 0$.

To simplify the theory a uniform value of M_p is desirable, therefore

$$M_p = (a+4m+1{,}25n')\cdot m_p \tag{3-32}$$

has been chosen.

The advantage of this value is that test results show that satisfactory results are obtained for design purposes.

An additional advantage is that in the case of collapse mechanism II the value of the sum of M_p and M_p' is equal to $(2a+8m+2{,}5n')\cdot m_p$, and therefore M_p' is also equal to $(a+4m+1{,}25n')\cdot m_p$.

Now the column flange can be considered as a T-stub flange with an *effective length* equal to $(a+4m+1{,}25n')$.

The equilibrium equations can be written as:

$$T\cdot m-(\hat{B}_t-T)\cdot n = (a+4m+1{,}25n')\cdot m_p \tag{3-33}$$

$$T\cdot m = 2(a+4m+1{,}25n')\cdot m_p \tag{3-34}$$

3.3 *The influence of stiffening plates*

The tests have shown that the deflections of a column flange in tension may be considerable.

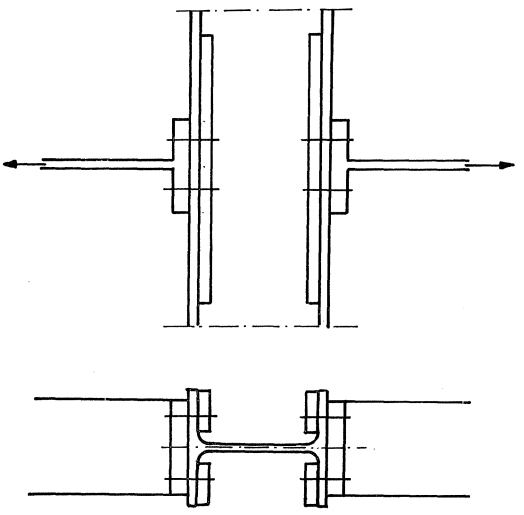

Fig. 3.9. Test specimen with stiffening plates.

Because the beam to column connection and the column flange in particular often determine the rigidity and strength of the whole structure a method is sought to stiffen or strengthen this flange.

Tests were executed with stiffening plates as shown in figure 3.9. Adopting the proposed design rules, which means that the column flange is considered as a T-stub with a length equal to $a+4m+1{,}25n'$, the calculation can be simple.

The value of M_p is not affected by the presence of the stiffening plates because the resisting bending moment is supposed to act at the line of the web.

It is assumed furthermore that no shear forces are present between the stiffening plates and the column flange, hence

$$M'_p = (a+4m+1{,}25n')\cdot(m_{p1}+m_{p2})$$

where m_{p1} is the yield moment per unit length of the column flange and m_{p2} is the yield moment per unit length of the stiffening plate.

Using this value of M'_p, the design of connections with stiffening plates reduces to a simple design method and the previously derived formulas can be applied

$$T\cdot m-(\Sigma\hat{B}_t-T)\cdot n \leqslant M_p \tag{1-5}$$

and

$$T\cdot m \leqslant M_p+M'_p \tag{1-6}$$

Whether the use of the simple design rules for stiffened column flanges is correct requires an analytical and/or experimental justification. Starting from collapse mechanism I, as shown in figure 3.3, the yield moments of yield lines 2 and 3 are increased with the yield moment of the stiffening plate.

As an illustration the collapse mode and the energy equation of mechanism I are given see figure 3.10 for the mode of collapse.

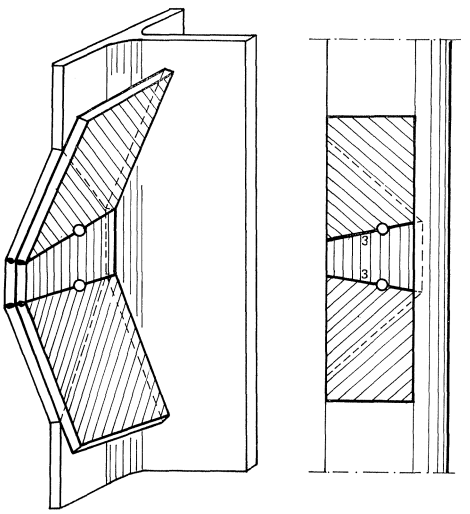

Fig. 3.10. The mode of collapse of mechanism I of the column flange with stiffening plates.

The energy equation of *collapse mechanism I* of the column flange *with stiffening plates* (bolt failure is the determining factor) is:

$$T \cdot \frac{m+n}{m} \cdot \Delta\delta = \left[\left\{ a + 2m \operatorname{tg}\alpha + 2(m+n) \frac{\cos\alpha}{\sin\beta \cdot \cos(\beta-\alpha)} + \right.\right.$$

$$\left. + 2(m+n') \frac{\sin\beta}{\cos\alpha \cdot \cos(\beta-\alpha)} \right\} m_{p1} +$$

$$\left. + \left\{ 2(m+n') \frac{\sin\beta}{\cos\alpha \cdot \cos(\beta-\alpha)} \right\} m_{p2} + \Sigma \hat{B}_t \cdot n \right] \cdot \frac{\Delta\delta}{m}$$

The test results show a satisfactory agreement with the proposed design rules, therefore a thorough analytical analysis has not been carried out.
The same considerations apply to mechanism II.
The energy equation and the mode of collapse of mechanism II are given as an illustration only. See figure 3.11 for the mode of collapse.

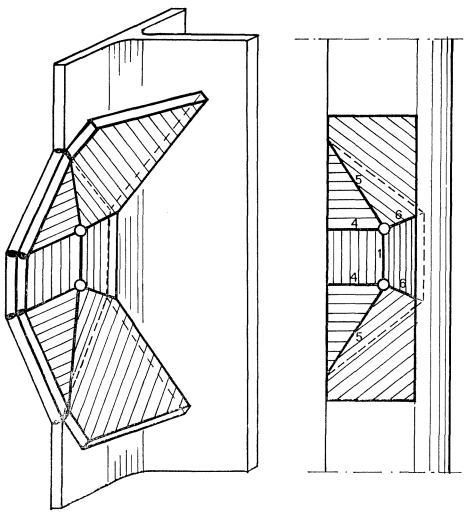

Fig. 3.11. The mode of collapse of mechanism II of the column flange with stiffening plates.

The energy equation of *collapse mechanism II* of the column flange *with stiffening plates* (collapse of the flange is the determining factor) is:

$$T \cdot \Delta\delta = \left[2 \left\{ \frac{a}{m} + \frac{m+2n'}{m} \frac{\cos\alpha}{\sin\beta \cdot \cos(\beta-\alpha)} + \operatorname{tg}\alpha + \operatorname{ctg}\beta + \frac{\sin\beta}{\cos\alpha \cdot \cos(\beta-\alpha)} \right\} m_{p1} + \right.$$

$$\left. + \left\{ \frac{a}{m} + 2\operatorname{ctg}\beta + \frac{2n'}{m} \frac{\cos\alpha}{\sin\beta \cdot \cos(\beta-\alpha)} + \frac{2\sin\beta}{\cos\alpha \cdot \cos(\beta-\alpha)} \right\} m_{p2} \right] \cdot \Delta\delta$$

Summarizing: Column flanges in tension with or without stiffening plates can be designed as T-stub flanges with an *effective length* equal to $(a+4m+1{,}25n')$.

The design formulas are:

$$T \cdot m - (\Sigma \hat{B}_t - T) \cdot n \leqslant (a+4m+1{,}25n') \cdot m_{p1}$$

$$\text{with } \Sigma \hat{B}_t - T \geqslant 0 \quad \text{else} \quad T = \Sigma \hat{B}_t \tag{3-35}$$

(bolt failure is the determining factor)

$$T \cdot m \leqslant (a+4m+1{,}25n') \cdot \{m_{p1} + (m_{p1} + m_{p2})\} \tag{3.36}$$

(collapse of the column flange is the determining factor).

where

m_{p1} = yield moment per unit length of the column flange
m_{p2} = yield moment per unit length of the stiffening plate
$\Sigma \hat{B}_t$ = the total design strength of the bolts fitted at one side of the column.

a, m and n' are parameters as given in the adjacent figure 3.12.

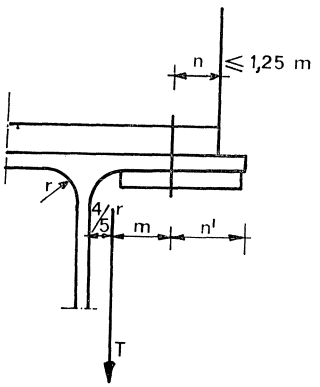

Fig. 3.12. Parameters of equations (3-35) and (3-36).

The smallest value of T obtained from the above mentioned formulas is the design strength of a column flange in tension.

The formulas show that it can be important to stiffen the flange if the collapse mechanism of the structure is governed by the collapse of the column flange. If, on the other hand, these calculations show that bolt fracture governs the structural collapse a bolt with a larger T must be chosen.

4 Test results

4.1 *Tests to check T-stub design*

Four tests were executed to check the theory developed for the design of T-stubs (see figure 4.1).

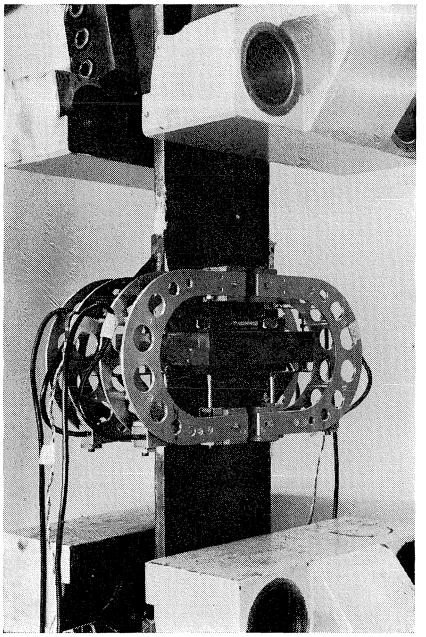

Fig. 4.1. Tests pecimen with equipment to measure the bolt forces.

In all test specimens failure due to the formation of mechanism A was observed.

In the experiments, therefore, bolt fracture was the determining factor; a calculation predicts the same result.

The test results are summarized in table I.

Table I

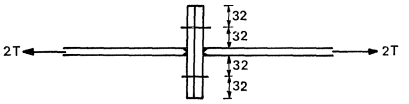

test no.	plate thickness in mm	σ_e N/mm²	$2\times\Sigma\hat{B}_t = 1{,}4\times\Sigma B_u$ kN	calculated $2T(\gamma=1{,}5)$ kN	fracture load kN	ratio between fracture load and calculated load	safety factor	mechanism
1	17	357	485	371,4	560	1,51	2,26	A
2	20	364	470,6	417,4	635	1,52	2,28	A
3	25	282	504,2	472,4	656	1,39	2,08	A
4	32	272	474,8	474,8	658	1,39	2,08	A

Table I shows that the safety factor against failure is sufficient ($\gamma > 2$).

4.2 *Tests to check the effective length*

Nineteen tests were executed to check the theory developed for the design of column flanges in tension.

A typical specimen is shown in figure 0.7 and figure 4.2.

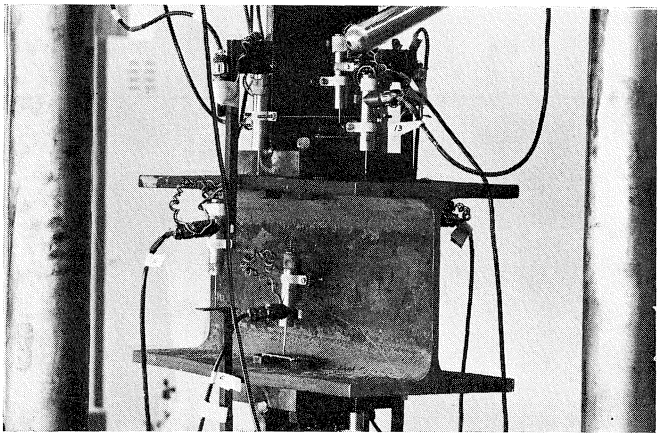

Fig. 4.2. Tests pecimen with equipment to measure the deformations of the flanges.

The T-stub flanges used have a thickness $t = 32$ mm and a bolt distance $a = 80$ mm.

The thickness of the T-stub flange is such that only elastic deformations occur.

The part of the specimen which represents the column is manufactured from European sections.

The dimensions of the specimens and the test results are summarized in table II.

If it is determined experimentally that the mode of failure is that of collapse mechanism I, (bolt failure), then this test result can be directly used to check the design viz the safety factor.

For collapse mechanism II, however, (yielding of the column flange) direct failure will not be observed and the load-deformation diagram must be used to obtain an indication of the real collapse load.

For all cases where collapse of the column flange is the determining factor such diagrams are given in figure 4.3.

The calculated values of the collapse loads are indicated in these diagrams. A typical example of a load-deformation diagram of a test specimen which fails by bolt fracture is given in figure 4.4 (specimen 21).

The following remarks can be made with respect to table II.

Tests 5 through 12 were performed to insure the validity of the developed theory.

The bolt of these test specimens were tightened up to the preload. Tests 13 and 14 were executed to investigate the influence of tightening while tests 15 through 19 were executed to justify the assumptions made in the design of stiffened column flanges.

Table II

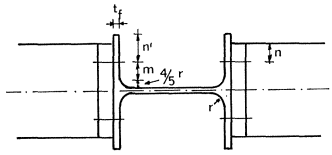

test no.	standard section HE	m mm	n' mm	n mm	t_f ●● mm	σ_e N/mm²	$2\times\Sigma B_t = 2\times 0.7\times \Sigma B_u$ kN	highest test load kN	$2T$ calculated with formula (3–35) ●●● kN	(3–36) ●●● kN	safety factor	collapse mechanism + remarks
5	140 A	33	24.5	24.5	8	260	490	220	244	122	–	II
6	140 A	23	34.5	28.75●	8	260	490	300	307	156	–	II
7	160 A	33	32	32	8.5	267	490	300	280	147	–	II
8	160 B	33	31	31	12.5	288	512	600	336	342	2.67	I bolt failure
9	160 B	23	41	28.75●	12.5	288	512	600	382	437	2.35	I bolt failure
10	160 M	29	35	32	23	270	484	660	484	1310	2.04	I bolt failure
11	200 B	33	48.5	28.5	15	300	512	560	387	558	2.17	I bolt failure
12	240 B	26	72	32	17	300	476	679	467	914	2.18	I bolt failure
13	140 A	33	24.5	24.5	8	260	490	220	244	122	–	II
14	140 A	33	24.5	24.5	8	260	490	180	244	122	–	II
15*	160 A	33	32	32	8.5	267	490	350	279	243	>2.16	II test load too low
16*	160 A	33	32	32	8.5	267	490	410	279	362	2.21	I bolt failure
17*	160 A	33	32	32	9.5	307	498	452	299	426	2.26	I bolt failure
18*	160 A	33	32	32	9.5	307	498	458	299	426	2.29	I bolt failure
19*	160 A	33	32	32	9.5	307	498	458	299	426	2.29	I bolt failure
20	200 B	33	48.5	28.5	14.5	210	507	535	333	365	2.41	I bolt failure
21	200 B	33	48.5	28.5	14.5	210	507	458	333	365	2.06	I bolt failure
22	200 B	33	48.5	28.5	14.5	210	463	495	313	365	2.38	I bolt failure
23	200 B	33	48.5	28.5	14.5	210	463	570	313	365	2.73	I bolt failure

* With stiffening plates

test no.	length mm	t mm	σ_e N/mm²
15	250	10	250
16	250	15	250
17	180	15	250
18	250	15	250
19	350	15	250

●: $n \leqslant 1.25$ m (according to McGuire – Steel structures)

●●: actual thickness

●●●: (3–35) $T\cdot m-(\Sigma\hat{B}_t-T)n \leqslant 2(a+4m+1{,}25n')\cdot m_p$

$\Sigma\hat{B}_t-T \geqslant 0$ else $T=\Sigma\hat{B}_t$

(3–36) $T\cdot m \leqslant (a+4m+1{,}25n')\times(2m_{p1}+m_{p2})$

where

m_{p1} = yield moment per unit length of the column flange

and

m_{p2} = yield moment per unit length of the stiffening plate

Figure 4.3a shows that the stiffness of the connection increases with the tightening of the bolts.

Figure 4.5 shows that the presence of stiffening plates increases the strength and stiffness of the connection considerably.

It is also obvious from the results of tests 17 through 19 that the length of the stiffening plate has only a small influence on the collapse load.

The large deformations of the column flange causes bending of the bolts which introduces additional tensile stresses in these bolts.

If this occurs in the threaded part of the bolt, the collapse load may decrease. To

examine the influence of this bending effect, tests 20 through 23 were executed.

In test specimens 21 and 22 the threaded part of the bolt was on the non-rigid side (flange side), while in specimens 20 and 23 the threaded part of the bolt was situated on the T-stub side.

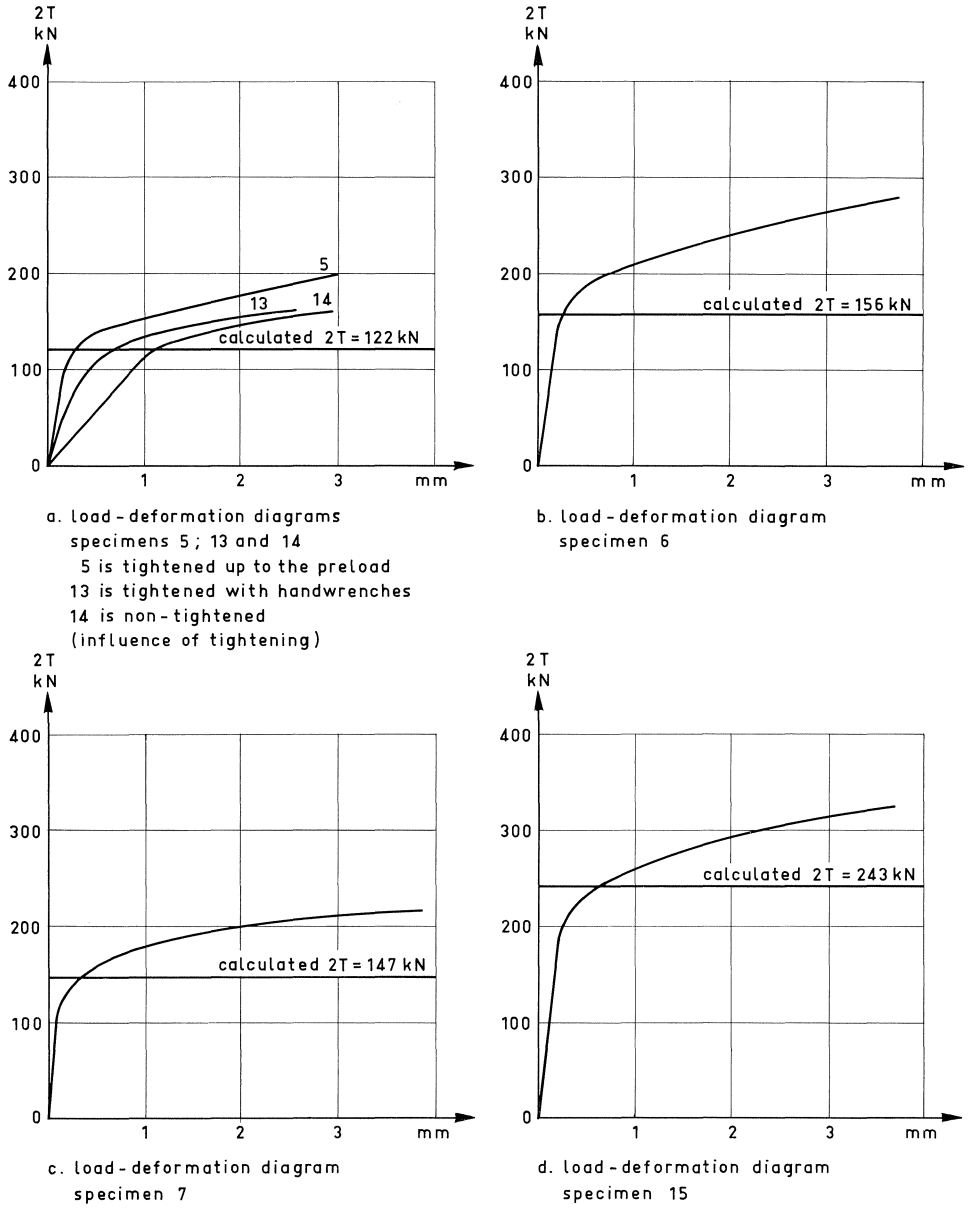

Fig. 4.3. Load-deformation diagrams of test specimens where collapse of the column flange is the determining factor (collapse mechanism II).

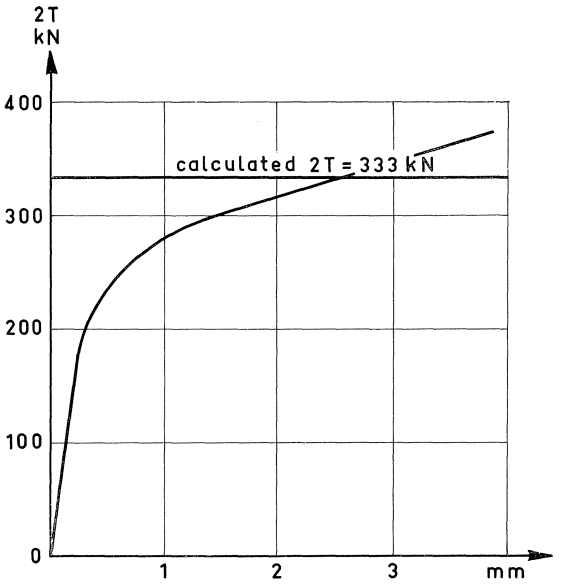

load-deformation diagram
specimen 21
(bolt failure is the determining factor)

Fig. 4.4

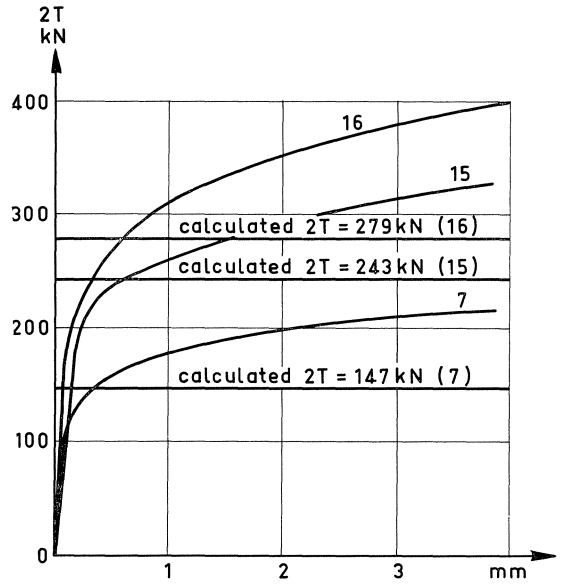

load-deformation diagrams
specimens 7, 15 and 16
(influence of stiffening plates)

Fig. 4.5

Despite of the clear influence of the bending stresses all specimens have a sufficient safety factor.

4.3 *Tests to check T-stub flange to column connection design*

Five tests were executed to check the philosophy that the design method of T-stubs can be applied also to connections where either the T-stubs or the column flange can collapse.

The test results and specimen dimensions are summarized in table III.

Table III

test no.	test specimen	plate thickness T-stub mm	calculated $2T$ T-stub mech. A kN	T-stub mech. B kN	column fl. mech. I kN	column fl. mech. II kN	$2\times\Sigma\hat{B}_t = 2\times0{,}7\times\times\Sigma B_u$ kN	fracture load	safety factor	determ. mech.
24	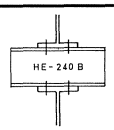	17	371.4	516	472	914	485	595	2.40	A
25		20	423	728	471	914	482	653	2.31	A
26		25	456	881	464	914	471	650	2.14	A
27	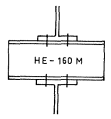	20	453	728	542	1310	542	680	2.25	A
28		25	479	881	517	1310	517	709	2.22	A

The test specimens were made of the same material as test specimens 10 and 12. The T-stubs were made of the same plate material as specimens 1 through 4.

The test results, summarized in table III, can therefore be compared with the calculated values $2T$ of table I and II when collapse of the flange is the determining factor.

If, however, fracture of the bolts is the determining factor, the calculated value of $2T$ must be adjusted because different bolts were used with another actual fracture load. Table III shows that the column flanges were rigid with respect to the T-stub flanges. The plastic deformations of specimen 12 together with the deformations of specimen 24 and 26 as shown in figures 4.6a, 4.7a and 4.8a, clearly indicate that the philosophy developed in chapter 2 is applicable.

The adjacent figures 4.6b, 4.7b and 4.8b give the position of the prying force Q.

Because the discussed theories are based on the existence of a prying force Q which causes an increase of the bolt force, the bolt forces of several test specimens were measured.

When the applied load of each bolt is plotted against the measured bolt tension a diagram as shown in figures 4.9 and 4.10 is obtained.

These figures clearly show the presence of a prying force Q.

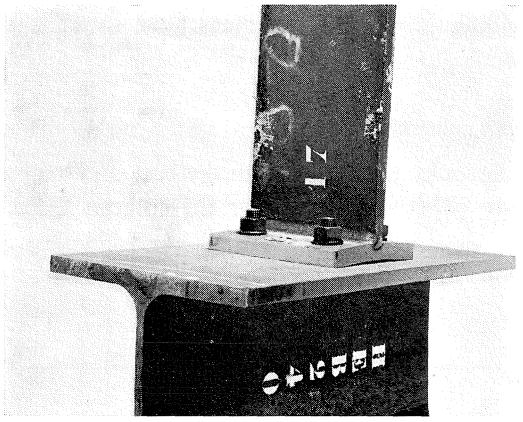

Fig. 4.6a. Plastic deformations of specimen 24.

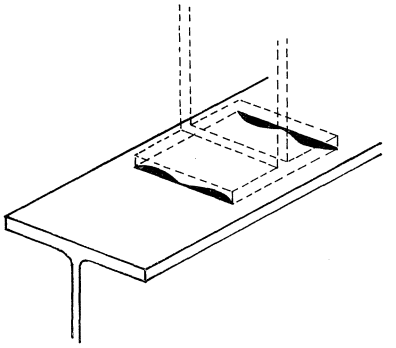

Fig. 4.6b. The location of prying force Q specimen 24.

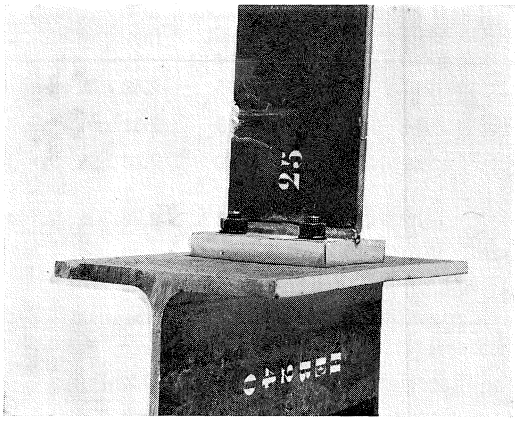

Fig. 4.7a. Plastic deformations of specimen 26.

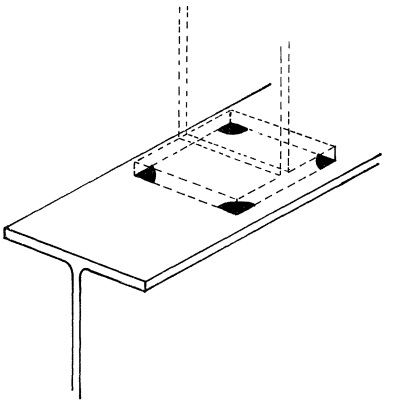

Fig. 4.7b. The location of prying force Q specimen 26.

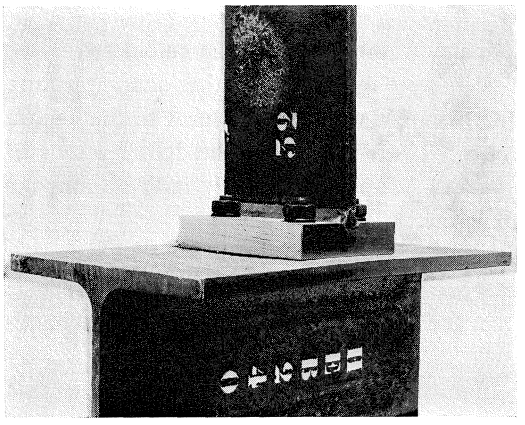

Fig. 4.8a. Plastic deformations of specimen 12.

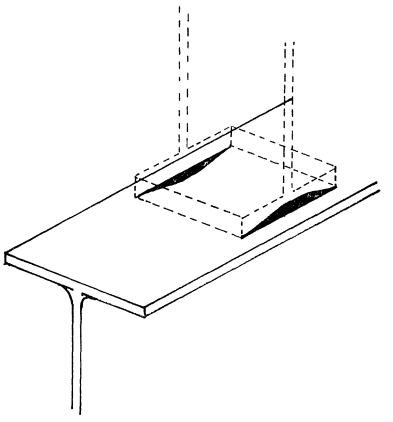

Fig. 4.8b. The location of prying force Q specimen 12.

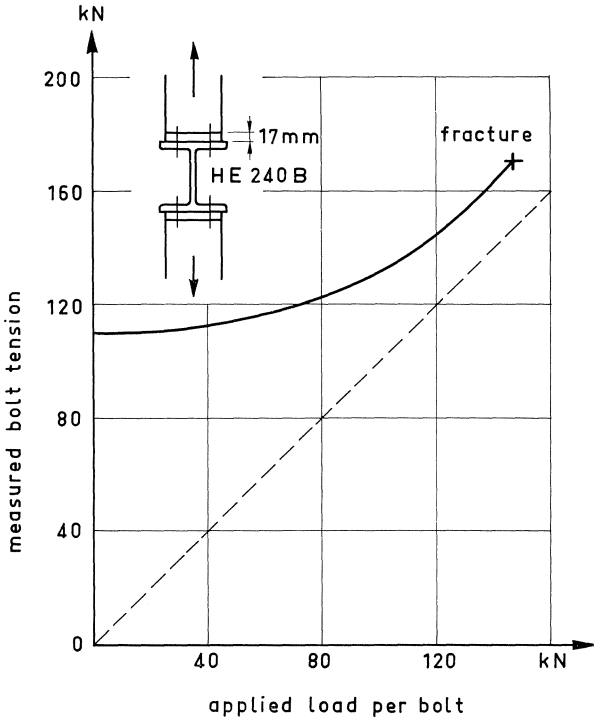

Fig. 4.9. Bolt tension versus applied load.

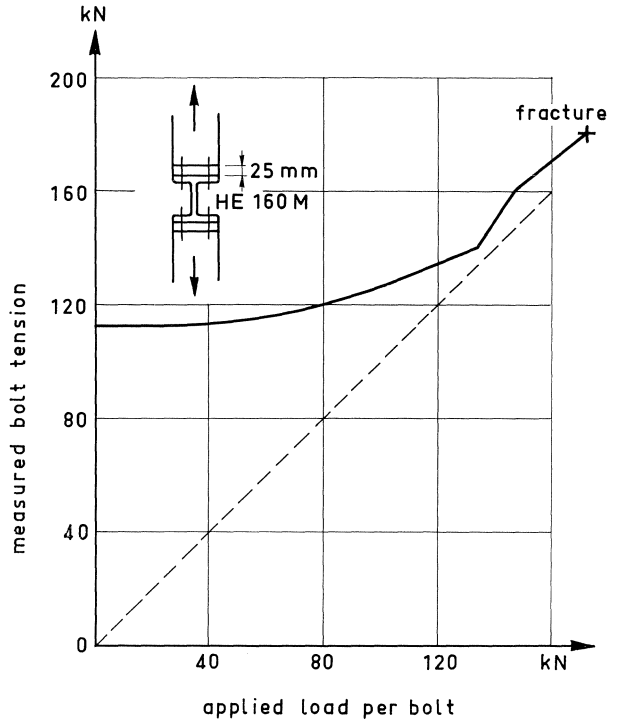

Fig. 4.10. Bolt tension versus applied load.

5 Deformations

The theories developed in the preceding pages are based on the limitations imposed by the strength of the materials of the connection. However, the deformations of the connections (the rotations) are also important in determining the behaviour of the structure as a whole.

These rotations have to be studied in the serviceability limit state as well as in the limit state of collapse.

Theoretically, three limitations on the rotations can be introduced.

1. In the serviceability limit state, the rotations should not be too large. Large rotations cause large deformations in the structure and these deformations may become the determining factor.
2. If the theory of plasticity is used and if the connections are made in redundant systems, then a necessary requirement is that in the limit state of collapse the rotations are large enough to allow the formation of plastic hinges in other parts of the structure.
3. When the ultimate design load is reached, the rotation of the connections should not be too large, because otherwise the overall deformation of the structure will be so large that one has to conclude that the structure has collapsed already before reaching the ultimate load of the connection. Bakker [1] has worked out these *three limitations on the deformations* as allowed in the T.G.B. Staal and according to the deformation capacity necessary to apply the theory of plasticity.

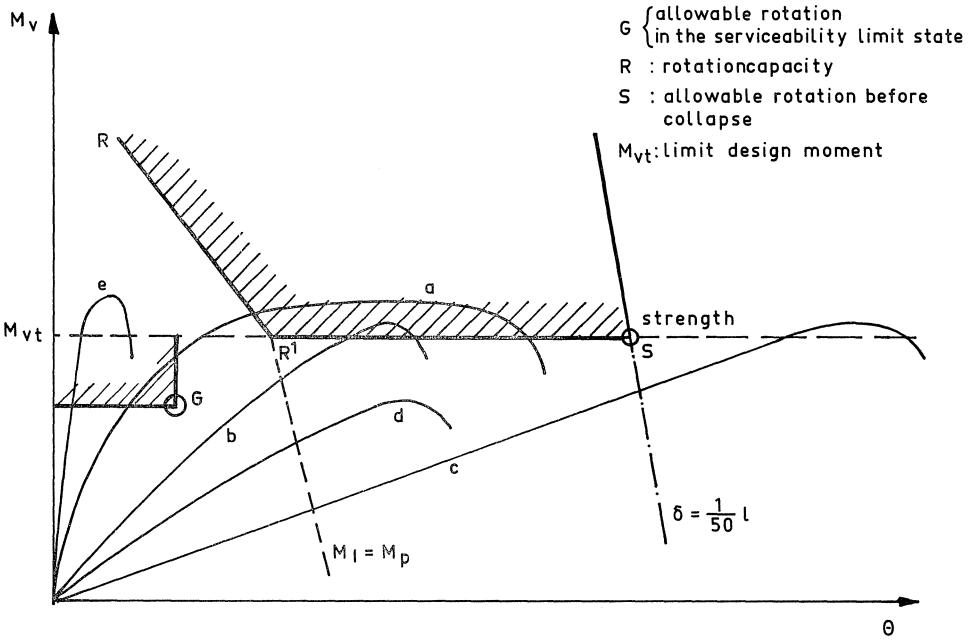

Fig. 5.1. Limitations on the rotations of beam-to-column connections.

He developed a graph which shows these limitations. An example of such a graph is given in figure 5.1.

The point G represents the maximum allowable rotation in the serviceability limit state (limitation 1). The line $R-R'$ gives the minimum required rotation before collapse (limitation 2) and the point S represents the maximum rotation before reaching the limit design load (limitation 3). A moment-rotation diagram of a connection must pass through the shaded areas in order to satisfy these limitations.

Only diagram, a, in figure 5.1 fulfils these requirements.

To check the moment-rotation behaviour of connections designed according formulas (3-35) and (3-36), twenty-three bolted moment connections were tested as shown in figure 6.1 and 6.2.

6 Tests to check the deformation limitations

6.1 *Introduction*

Twenty-three bolted moment connections were tested as shown in figure 6.1 and 6.2.

In this chapter these test results are discussed in order to demonstrate that the

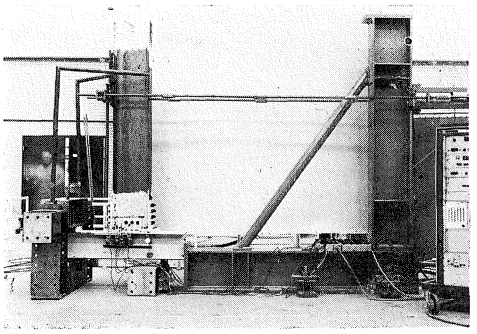

Fig. 6.1. Overall view of the test set up.

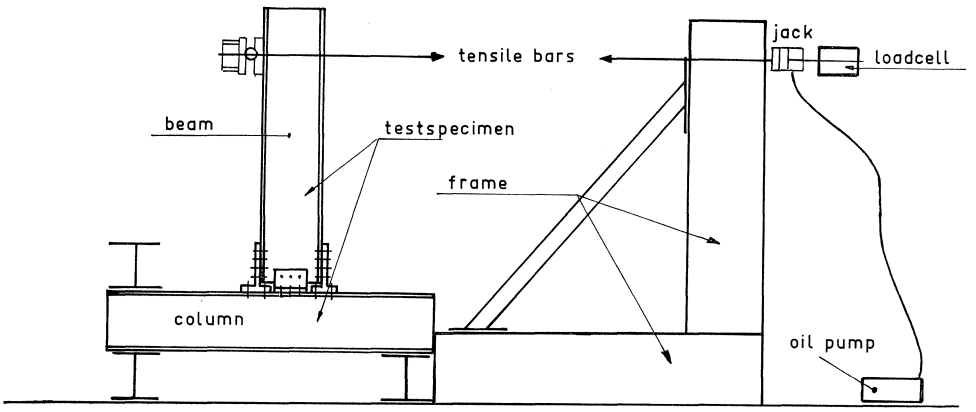

Fig. 6.2. Testing scheme.

requirements of the moment-rotation diagrams are satisfied if the test specimens are designed in accordance with formulas (3-35) and (3-36).

The connections are designed in such a way that collapse of the column flanges is the determining factor. Ten specimens have column sections HE 200 A and beam sections IPE 300.

The other thirteen specimens have column sections HE 300 A and beam sections IPE 400.

The differences between the various connections and also the test results are given in the tables IV and V.

In the next a brief description of the test specimens is given.

Specimen:	*Description:*
1 and 3 through 7 11 and 13 through 18	T-stub connections with web connectors of steel angles.
8, 12, 19 and 23	T-stub connections without web connectors
2 and 22	end plate connections not extended beyond the tension flange
9, 10, 20 and 21	end plate connections.

The flange of test specimens 5, 7, 8, 10, 12, 14, 15, 19, 21 and 22 are stiffened with bolted plates parallel to the flanges while specimens 6 and 16 have stiffening plates welded between the flanges.

The bolts of specimens 3 and 13 are tightened up to the preload. The other bolts of the specimens are tightened with hand wrenches.

6.2 *Explanation to the results mentioned in table IV and V*

For each specimen the moment-rotation diagram is determined.

The *yield moments corresponding to the limit states of deformation* as discussed in chapter 5 are obtained by assuming that the points G and/or S (of figure 5.1) lie on the corresponding moment-rotation diagram.

To do so it is necessary to adopt a hypothetical beam length, as shown in [1]. In this case this length has been chosen to be 30 or 40 times the height of the beam.

For the yield stress of the beam the theoretical value of $\sigma_e = 240$ N/mm^2 has been used.

For other parts of the specimen the actual yield stress has been determined. The values obtained from the moment-rotation diagram can now be compared with the theoretical yield moment of the connection (M_{vt}) calculated according to the plate buckling formulas of the T.G.B. 1972–Staal as well as with the theoretical yield moment of the connection (M_{vt}) calculated using formula (3-36) given in chapter 3.

The latter value of M_{vt} is obtained by multiplying the limit state load, of the column flange in tension $2T$, by the center distance of the beam flanges. For the specimens with an end plate connection not extended beyond the tension flange (2 and 22), the distance between the center of the bolts in tension and the compressed beam flange is used.

It is assumed that the bolts and that part of the end plate which is symmetrical about the tension flange of the beam can be treated as an equivalent T-stub connection and can be designed according to the methods proposed previously for T-stub connections.

This assumption is made in agreement with a suggestion of W. McGuire [2]. A possible objection to this method can be that the limit state load $2T$ should be multiplied by the center distance of the T-stubs instead of by the center distance of the flanges. In that case, the values of M_{vt} will increase by about 8% with respect to the previous mentioned values.

Another questionable assumption is that the bending moment carried by the web connectors is neglected. The tests revealed this bending moment to be present. A correct method to take this bending moment into account has not yet been found.

The design formulas (3-35) and (3-36) are on the safe side if the calculated values of M_{vt} are smaller than the values obtained from the moment-rotation diagrams. This implies that the calculated limit state of collapse is reached before the limit state of deformations.

The tests of tables IV and V show formula (3-36) to be correct in all cases where the beam span in a braced frame is equal to 30 times the beam height (with the exception of specimen 12).

In the cases however where the beam span is 40 times the beam height, formula (3-36) does not always holds true.

This means that the proposed design method is not applicable for beams with spans larger than 30 times the beam height.

For longer spans a test must be executed to determine the limit states of deformation.

In the tables IV and V buckling results are also mentioned because these results were obtained simultaneously; they will not be discussed here however. Figure 6.3 shows why test specimen 12 of table V did not reach the expected yield moment.

The tension side of the connection was fabricated as two separated T-stubs, each of which connects half of the beam flange.

The T-stub webs yielded due to the reduced stiffness and due to the effect of prying force Q.

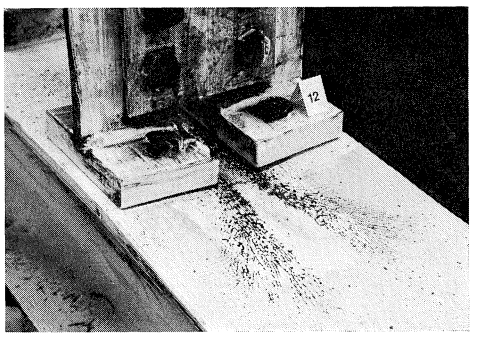

Fig. 6.3. The plastic deformations of specimen 12 of table V.

Table IV

Column: HE200A — Beam: IPE 300 — Bolts: M20–10.9
$\sigma_e = 262$ N/mm² — $EI = 17600$ kNm²
$t_f = 10$ mm — $M_p = 150{,}7$ kNm ($\sigma_e = 240$ N/mm²)
all bending moments are given in kNm

test no.	specimen	highest test load	yield moment corresponding to the limit states of deformations obtained from moment-rotation diagram			M_{vt} calculated with buckling formulas and formula (3–36)		remarks (buckling observed)
			G beam span 9 m	G beam span 12 m	S	buckling TGB 1972 Staal	formula (3–36)	
END PLATE CONNECTIONS								
2		98	64	33	90	55	52	***
9		143	127	87	125	75	66	138**
10		152	160	123	150	75	112	122**
T-STUB CONNECTION WITHOUT WEB CONNECTORS								
8	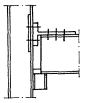	149	129	94	200	67	114	
T-STUB CONNECTION WITH WEB CONNECTORS								
1		167	129	96	150	76	67	150**
3	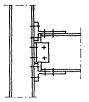	159	176	136	160*	76	67	130**
4	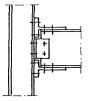	145	116	85	155*	76	67	bolts in tension are bolts M16 10.9
5		144	140	105	250*	76	114	132**
6		180	227	168	190*			
7		192	173	130	200*	76	114	167**

* values obtained by extrapolation
** connection moment where web buckling is observed
*** web buckling observed after testing

Table V (for continuation see page 52)

Column: HE300A — Beam: IPE 400 — Bolts: M22 10.9
$\sigma_e = 265{,}5$ N/mm² — $EI = 48600$ kNm²
$t_f = 14$ mm — $M_p = 313{,}9$ kNm ($\sigma_e = 240$ N/mm²)
all bending moments are given in kNm

test no.	specimen	highest test load	yield moment corresponding to the limit state of deformations obtained from moment-rotation diagram			M_{vt} calculated with buckling formulas of T.G.B. 1972 and formula (3–36)		remarks (buckling observed)
			G beam span 12 m	*G* beam span 16 m	*S*	buckling T.G.B. 1972 Staal	formula (3–36)	
END PLATE CONNECTIONS								
20	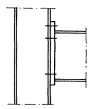	246	230	160	245	190	172	219**
21	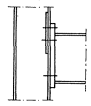	296	279	208	280	190	261	***
22	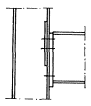	206	237	165	220*	145	160	***
T-STUB CONNECTIONS WITHOUT WEB CONNECTORS								
12	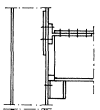	270	188	116	265	154	258	270** T-stubs separated
19	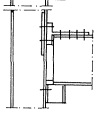	300	314	235	340*	154	258	***
23	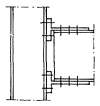	255	237	163	280*	204	170	

* values obtained by extrapolation
** connection moment where web buckling is observed
*** web buckling observed after testing

Table V (continuation)

Column: HE300A — Beam: IPE 400 — Bolts: M22-10.9
$\sigma_e = 265{,}5$ N/mm² — $EI = 48600$ kNm²
$t_f = 14$ mm — $M_p = 313{,}9$ kNm ($\sigma_e = 240$ N/mm²)
all bending moments are given in kNm

test no.	specimen	highest test load	yield moment corresponding to the limit state of deformations obtained from moment-rotation diagram			M_{vt} calculated with buckling formulas of T.G.B. 1972 and formula (3–36)		remarks (buckling observed)
			G beam span 12 m	G beam span 16 m	S	buckling T.G.B. 1972 Staal	formula (3–36)	
T-STUB CONNECTION WITH WEB CONNECTORS								
11	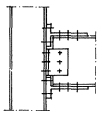	300	272	197	350*	204	170	294**
13	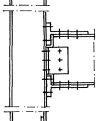	306	318	233	350*	204	170	***
14	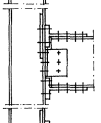	333	360	280	400*	204	258	327**
15	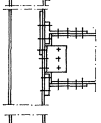	340	282	219	450*	204	258	327**
16	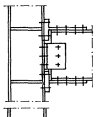	420	398	275	450*			stiffening plates between flanges
17	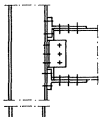	270	240	163	325*	204	144	width of column flange reduced $n = 35$ mm
18	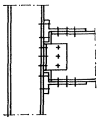	259	282	210	340*	199	87	270** column flange thickness made 10 mm

* values obtained by extrapolation
** connection moment where web buckling is observed
*** web buckling observed after testing

Figures 6.4, 6.5 and 6.6 give an impression of the large deformations which the test specimens endured.

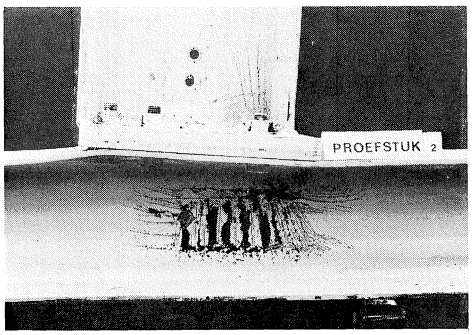

Fig. 6.4. The plastic deformations of test specimen 2 of ta le IV.

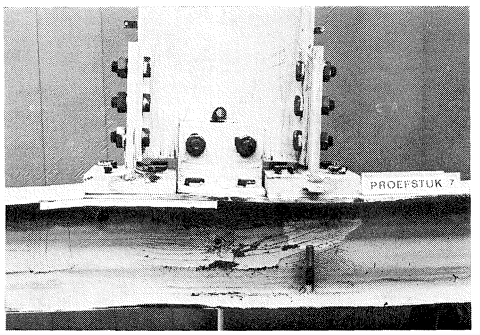

Fig. 6.5. The plastic deformations of test specimen 7 of table IV.

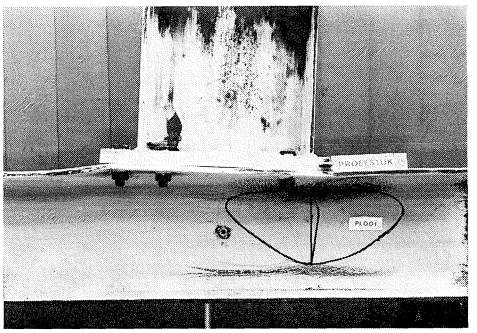

Fig. 6.6. The plastic deformations of test specimen 20 of table V (Plooi = web buckling).

An example of a moment-rotation diagram is given in figure 6.7. This diagram corresponds to test specimen 1 (see table IV).

The shaded areas are constructed in agreement with the design requirements given in the report of Bakker [1] by using the bending moment M_{vt} calculated with formula (3-36).

The yield moment which corresponds to the limit state of deformation (where the point G lies on the diagram), is also plotted in order to show how the values of tables IV and V were obtained.

6.3 *Additional tests*

The moment connections discussed in the above paragraph are composed of oversized T-stubs and end plates and therefore the test results do not give a realistic impression of the rotations which can occur when all parts of the connection are designed efficiently.

For that reason four additional tests were executed, as shown in figures 6.8 and 6.9.

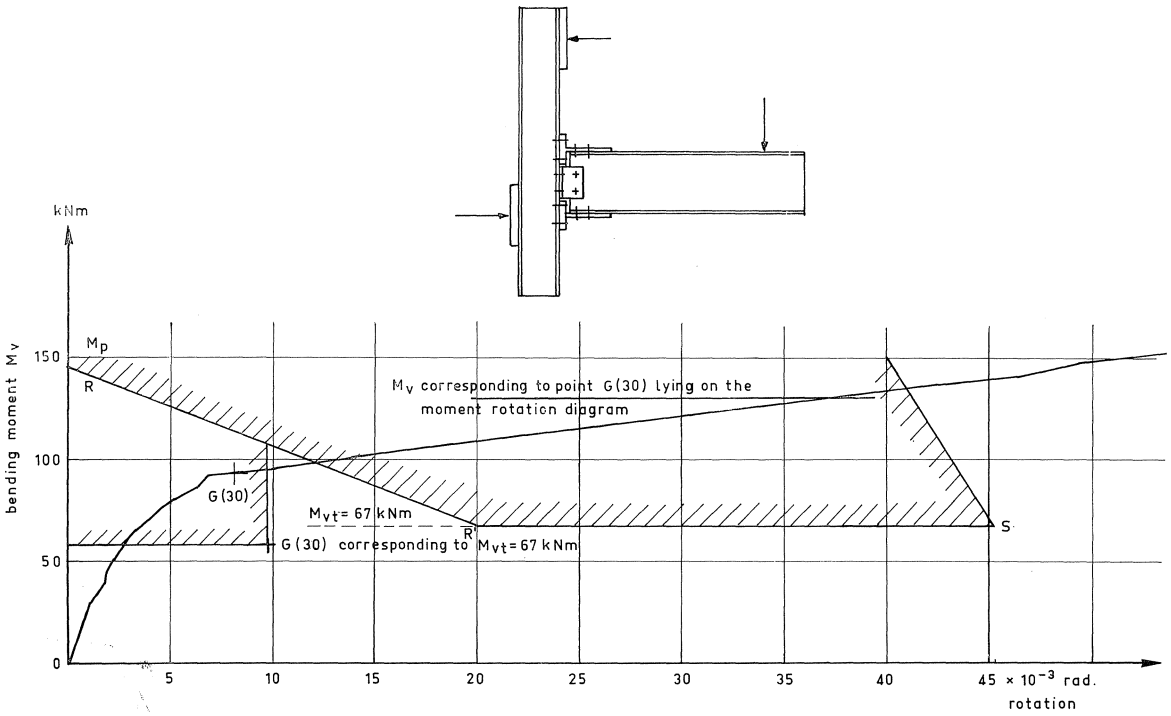

Fig. 6.7. Moment rotation diagram of test specimen 1 of tabel IV.

The frames are tested at actual size.

These tests show the behaviour of a steel frame loaded to failure with an increasing uniformly distributed load.

The connections in the frame are designed according the theories discussed in this paper.

The types of connections are shown in figure 6.10 through 6.16. Adjacent to these figures the moment-rotation diagrams with the limitations on the rotations are given for a beam span equal to 30 times the beam height.

These figures show also that the connections allow large deformations. The results obtained show that the design theory for T-stubs and column flanges in tension discussed herein is correct. When the beam span is smaller than or equal to 30 times the beam height the connections designed in accordance with this theory do not reach the limit state of deformations before reaching the limit state of collapse.

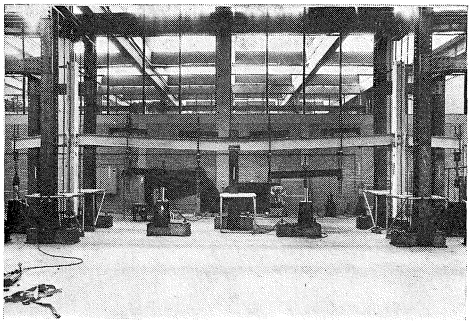

Fig. 6.8. Overall view of test set up of the steel frames.

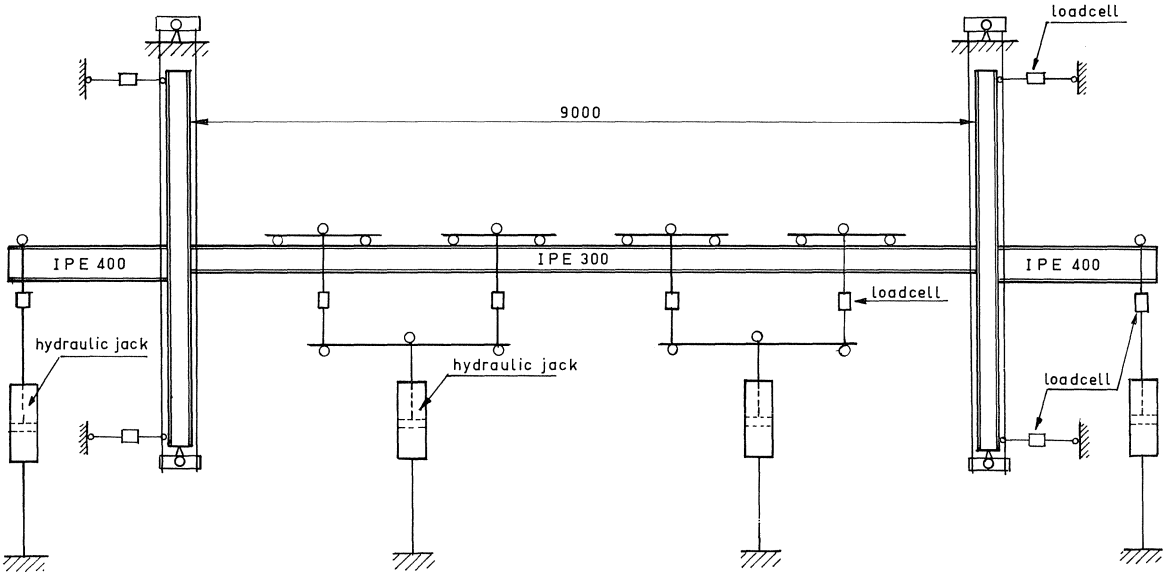

Fig. 6.9. Test set up of the steel frames.

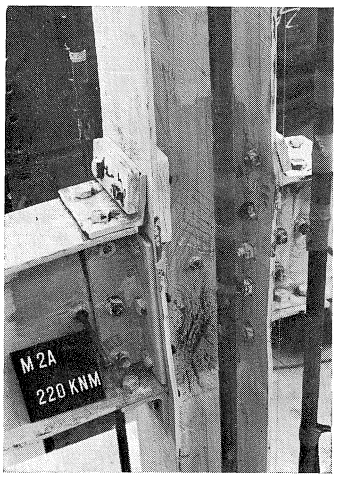

Fig. 6.10a. Plastic deformations of a beam-to-column connection designed with formula (3–35) and/or (3–36).

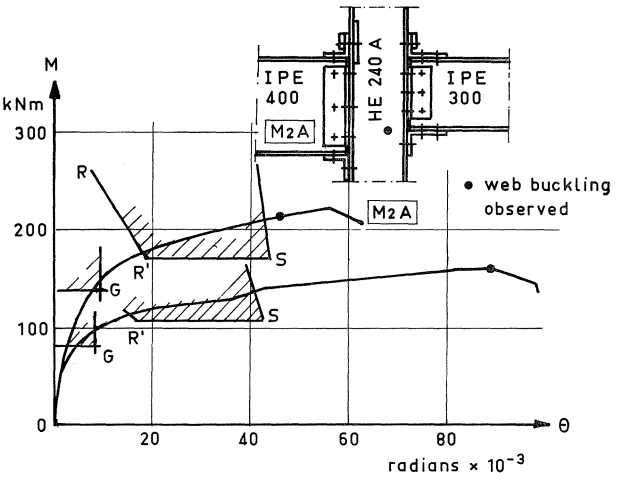

Fig. 6.10b. Moment-rotation diagram with the limitations on the rotations.

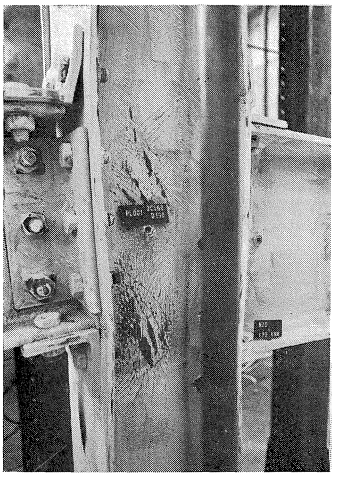

Fig. 6.11a. Plastic deformations of a beam-to-column connection designed with formula (3–35) and/or (3–36).

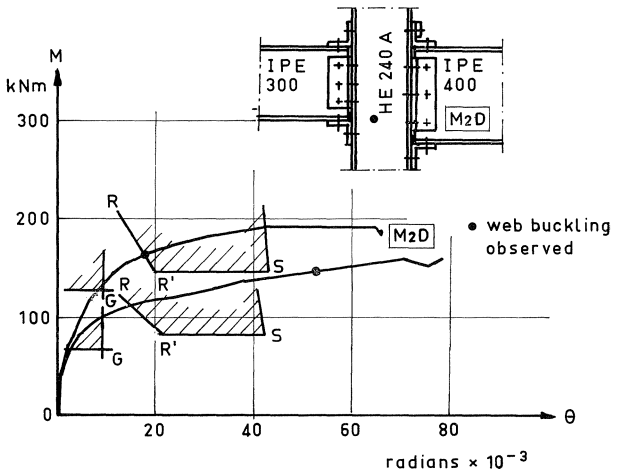

Fig. 6.11b. Moment-rotation diagram with the limitations on the rotations.

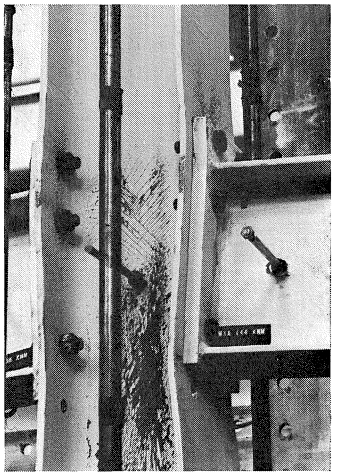

Fig. 6.12a. Plastic deformations of a beam-to-column connection designed with formula (3–35) and/or (3–36).

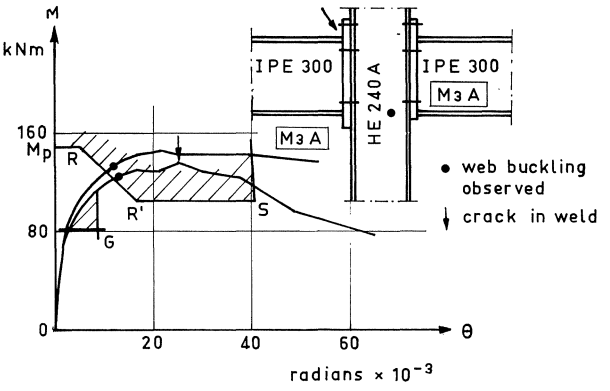

Fig. 6.12b. Moment-rotation diagram with the limitations on the rotations.

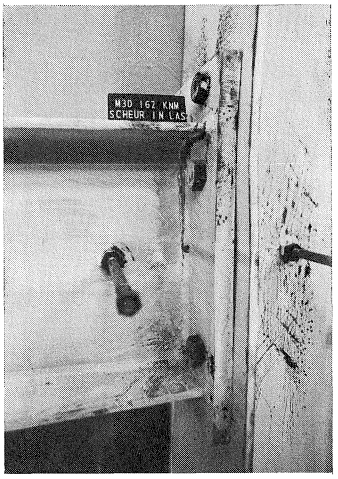

Fig. 6.13a. Plastic deformations of a beam-to-column connection designed with formula (3–35) and/or (3–36).

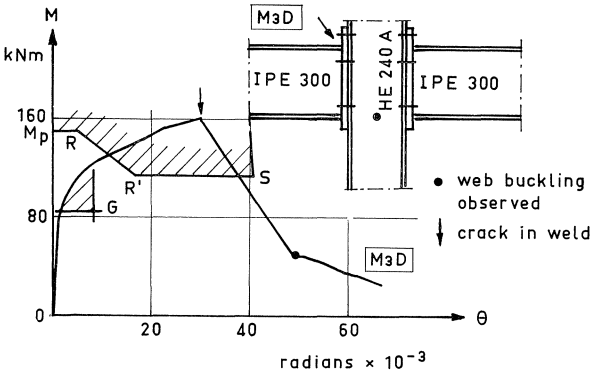

Fig. 6.13b. Moment-rotation diagram with the limitations on the rotations.

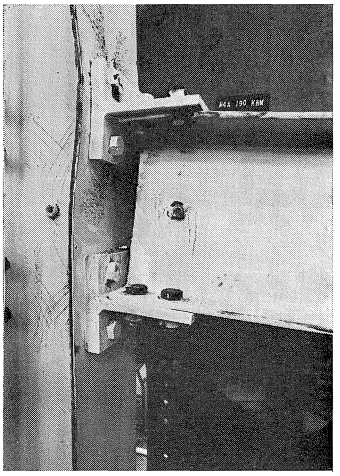

Fig. 6.14a. Plastic deformations of a beam-to-column connection designed with formula (3–35) and/or (3–36).

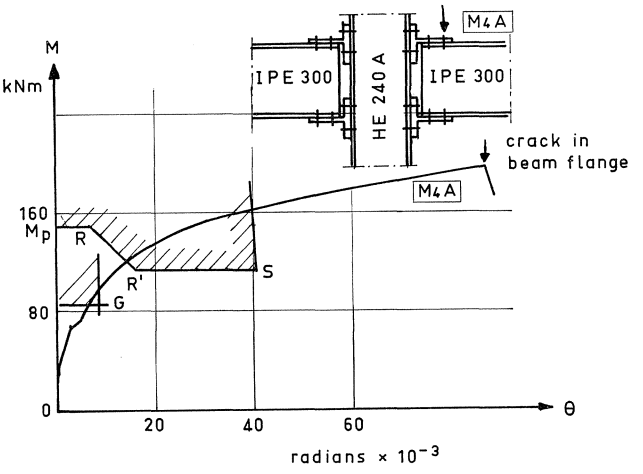

Fig. 6.14b. Moment-rotation diagram with the limitations on the rotations.

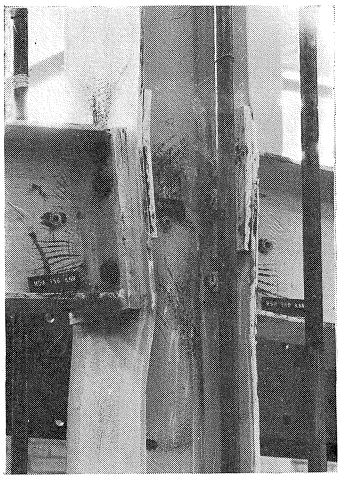

Fig. 6.15a. Plastic deformations of a beam-to-column connection designed with formula (3–35) and/or (3–36).

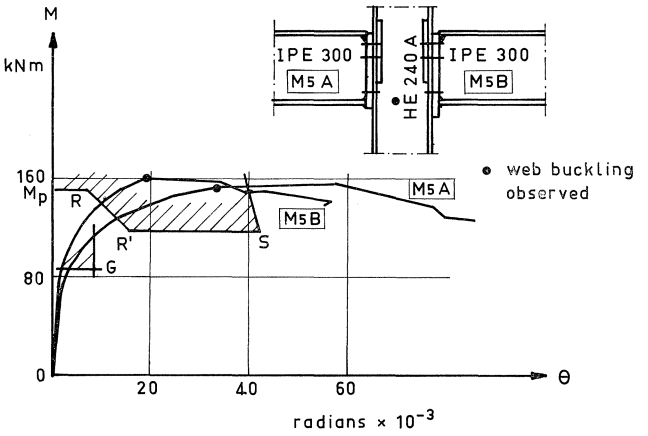

Fig. 6.15b. Moment-rotation diagram with the limitations on the rotations.

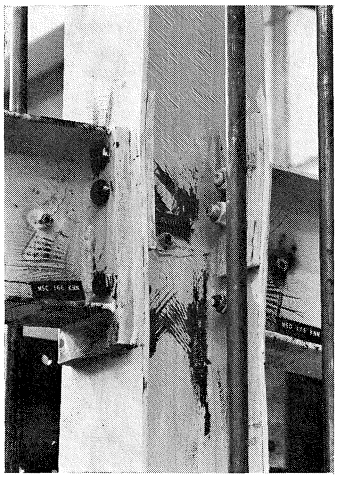

Fig. 6.16a. Plastic deformations of a beam-to-column connection designed with formula (3–35) and/or (3–36).

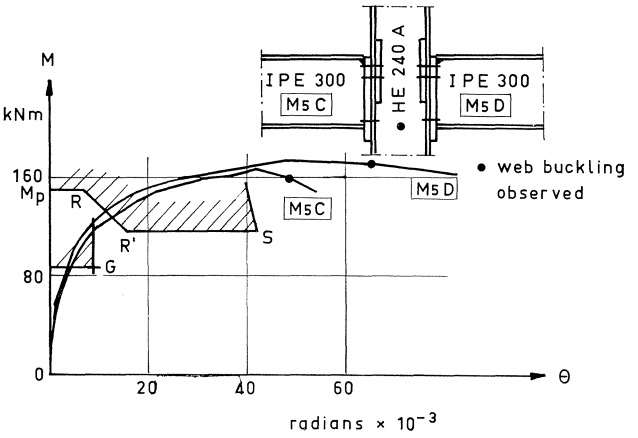

Fig. 6.16b. Moment-rotation diagram with the limitations on the rotations.

7 Concluding remarks

1. The tension side of statically loaded, bolted beam-to-column connections can be designed with formula (3-35) and (3-36).
   Formula (3-35) gives the design load if bolt failure governs collapse.
   Formula (3-36) gives the design load if collapse of the flange of the T-stub or the column is the determining factor (stiffened or not stiffened).
2. T-stub flange and column flange can be designed independent of each other.
3. For T-stub design *the effective length* $a+4m+1{,}25n'$ can not exceed the width of the T-stub flange.
4. The application of stiffening plates bolted parallel to the flanges is only significant in the case where collapse of the flanges is the determining factor.
5. Moment connections designed with the above-mentioned formulas and applied to beams in braced frames with spans smaller than or equal to 30 times the beam height fulfil the deformation requirements as stated in the T.G.B. 1972–Staal. The compression side should be checked separately.

References

[1] Bakker, C. Th. J., Eisen waaraan hoekverbindingen in staalskeletten moeten voldoen. T.N.O. Report Nr. BI-73-70 (1973).

[2] McGuire, W., Steel Structures. Prentice Hall, Inc./Englewood Cliffs, M.J., 1968.

[3] De Back, J. and P. Zoetemeijer, High strength bolted beam to column connections. The computation of bolts, T-stub flanges and column flanges. Stevin Report Nr. 6-72-13 (1972).